Isotopic identification of global nitrogen hotspots across natural terrestrial ecosystems

Edith Bai[1*], Benjamin Z Houlton[1], Ying Ping Wang[2]

[1]Department of Land, Air and Water Resources, University of California, Davis, California, USA.[2]CSIRO Marine and Atmospheric Research and Centre for Australian Weather and Climate Research, Aspendale VIC 3195, Victoria, Australia

*Corresponding information:

Edith Bai

State Key Laboratory of Forest and Soil Ecology,

Institute of Applied Ecology,

Chinese Academy of Sciences,

Shenyang 110164, China

Phone: +86-24-83970570

Fax: 530-752-1552

Email: baie@iae.ac.cn

Abstract

Nitrogen (N) influences local biological processes, ecosystem productivity, the composition of the atmospheric-climate system, and the human endeavour as a whole. Here we use natural variations in N's isotopes, coupled with two models, to trace global pathways of N loss from the land to the water and atmosphere. We show that denitrification accounts for approximately 35% of total N losses from the natural soil, with NO, N_2O, and N_2 fluxes equal to 15.7 ± 4.7 Tg N yr^{-1}, 10.2 ± 3.0 Tg N yr^{-1}, and 21.0 ± 6.1 Tg N yr^{-1}, respectively. Our analysis points to tropical regions as the major "hotspot" of nitrogen export from the terrestrial biosphere, accounting for 71 % of global N losses from the natural land surface. The poorly studied Congo basin is further identified as one of the major natural sources of atmospheric N_2O. Extra-tropical areas, by contrast, lose a greater fraction of N via leaching pathways (~77% of total N losses), than do tropical biomes, likely contributing to N limitations of CO_2 uptake at higher latitudes. Our results provide an independent constraint on global models of the N cycle among different regions of the unmanaged biosphere.

1. Introduction

Nitrogen (N) is essential to all life and affects many different aspects of the Earth system as a whole. At the molecular scale, for instance, N is a significant component of nucleic acids, protein and other biomolecules that regulate a suite of cell functions. At larger scales, N influences the climate system via its direct impact on climate forcing and indirectly via its role in constraining CO_2 uptake and storage on land and in the sea (Fig. 1). Consequently, biogeochemists, climatologists, and ecologists are fundamentally

interested in understanding how N cycles among Earth's biomes and across a spectrum space-time scales – especially in terms of how much N enters and leaves the biosphere along dissolved vs. gaseous paths.

However, two principal factors have greatly challenged this objective. First, N_2 – likely the dominant gaseous N product of soil bacteria – is difficult to measure accurately because of the large background concentration of N_2 in air (Scholefield et al., 1997;Swerts et al., 1995). This challenge has sparked controversies over the "missing N" in the global N budget (Galloway *et al.*, 2004). Second, emissions of NO, N_2O or N_2 can vary significantly in space and time; hence, scaling up field measurements, using either empirical or computational models, imparts large, unexplained errors in estimates of gaseous N emissions (Matson et al., 1989;Galloway et al., 2004;Scheer et al., 2009;Butterbach-Bahl et al., 2002;McClain et al., 2003;Groffman et al., 2009). Consequently, modeling has become an essential tool for estimation of N gas emissions at regional to global scales.

Boyer et al. (2006) reviewed current approaches for modeling terrestrial N gas fluxes at regional scales. The two basic approaches involve either mass-balance (Howarth *et al.*, 1996) or simulation models, particularly DAYCENT (Parton *et al.*, 1998), DNDC (denitrification-decomposition) (Li *et al.*, 1992), CASA (Carnegie-Ames-Stanford) (Potter *et al.*, 1996), EPIC (erosion-productivity impact calculator) (Williams *et al.*, 1984), and INCA (integrated nitrogen in catchment) (Whitehead *et al.*, 1998). These latter models build on various rate-controlling properties of denitrification such as climatic, soil, nutrient, and land use characteristics. They are generated to varying degrees from empirical measurements that are extrapolated from lab and field studies to

62 ecosystems, regions and the globe. However, due to the complexities in N
63 transformations, these models are generally highly parameterized and poorly constrained
64 by observations that integrate large scales of space and time. In addition, it is difficult to
65 obtain good estimates of many of the spatially heterogeneous variables used to constrain
66 denitrification and some input data are not available at the global scale (Groffman *et al.*,
67 2009).

68 Natural variations in N isotope abundance have provided insights into large-scale
69 N dynamics of ecosystems on land and in the sea (Amundson and Baisden, 2000;Houlton
70 et al., 2006;Handley et al., 1999;Brenner et al., 2001;Amundson et al., 2003;Houlton and
71 Bai, 2009;Bai and Houlton, 2009;Altabet et al., 1995;Sigman et al., 2003;Devol et al.,
72 2006;Morford et al., 2011). The stable isotopes of N, ^{15}N and ^{14}N, vary naturally in their
73 abundance among biogenic materials owing to isotope fractionations, particularly kinetic
74 ones, which are commonly associated with organisms' enzymatic preferences for
75 isotopically light N (^{14}N) (Kendall, 1998). Within the terrestrial biosphere, coherent
76 patterns in the N isotope composition of soils and ecosystems are observed across
77 gradients in temperature, precipitation, and latitude (Handley et al., 1999;Amundson et al.,
78 2003;Craine et al., 2009). Such $^{15}N/^{14}N$ patterns in total soil N pools reflect the dominant
79 pathways by which N enters and leaves ecosystems (Amundson et al., 2003;Houlton et al.,
80 2006;Bai and Houlton, 2009;Houlton and Bai, 2009). Houlton and Bai (2009) have
81 previously developed an isotopic approach to partition the N losses between gaseous and
82 leaching vectors for the natural land biosphere. However, their approach did not consider
83 regional-scale variations in N loss fractions, fluxes or forms; rather it envisaged the
84 natural terrestrial environment as a single vector. Here we extend on Houlton and Bai

85 (2009)'s approach by partitioning gaseous N losses into NO, N_2O and N_2 across different
86 sectors of the unmanaged land biosphere, thereby identifying the major natural hot spots
87 of leaching and denitrification (including NO, N_2O, and N_2) among regions. We then
88 compare our estimates with other independent estimates of N gaseous emissions based on
89 past analyses, including process-based modeling, statistical modeling, mass-balance
90 calculations and satellite-based approaches.

91 **2. Materials and methods**

92 Our approach involves three phases (Fig. 2). First, we use estimates of the N isotope
93 composition of soil to constrain the proportion of N lost to denitrification vs. leaching
94 paths across different terrestrial ecosystems. Second, we use two separate models to
95 provide spatially explicit estimates of N fixation (Wang and Houlton, 2009) and N
96 deposition inputs (Lelieveld and Dentener, 2000) and thereby convert our N loss
97 proportions to steady-state fluxes. Third, we use a simple model to further partition
98 denitrification gases into N gas fates, including NO, N_2O and N_2. In the case of NO, we
99 compare the modeled results to satellite-based estimates of NO_2 emissions over the
100 continent of Africa.

101 **2.1 Nitrogen isotope model**

102 N isotope ratios are presented in delta notation:

103 $$\delta = [(R_{sample} - R_{STD}) / R_{STD}] \times 10^3 \quad (1)$$

104 where R_{sample} is the $^{15}N/^{14}N$ ratio of the sample and R_{STD} is the $^{15}N/^{14}N$ ratio of the
105 atmospheric dinitrogen.

Our N isotope model is based on the conceptual model of controls on whole-ecosystem $^{15}N/^{14}N$ (Houlton *et al.*, 2006). Although plant uptake can discriminate against ^{15}N when N is abundant (Evans, 2001), the expression of this isotope effect is not observed in many natural sites where N is scarce (Houlton et al., 2007). More likely are isotope effects owing to mycorrhizal symbionts, which can deliver low $^{15}N/^{14}N$ compounds to hosts, potentially causing leaves to have a lower $\delta^{15}N$ than the soils on which plants rely (Hobbie and Hobbie, 2006;Craine et al., 2009). Nevertheless, regardless of any such isotope effect, plant and associated root symbionts return N to the soil with the same weighted $\delta^{15}N$ as that of N uptake as these systems approach the steady-state. Therefore, under steady state conditions, internal N cycling processes (plant uptake and microbial uptake) do not influence bulk soil $^{15}N/^{14}N$ ratios because they are recycling N as opposed to affecting overall N balances (Bai and Houlton, 2009;Brenner et al., 2001;Houlton et al., 2006). This lack of internal N cycle control on $^{15}N/^{14}N$ has been proven mathematically (Brenner et al., 2001;Amundson et al., 2003;Houlton et al., 2006;Bai and Houlton, 2009) and is supported by empirical observations across a broad range of climatic and ecosystems conditions (Bai and Houlton, 2009;Houlton et al., 2006;Houlton and Bai, 2009). Although further inquiry into potential plant and microbial recycling effects on ecosystem $^{15}N/^{14}N$ would be useful in general (see discussion), we here apply the steady-state assumption as a first approximation, consistent with other global biogeochemical modeling efforts (Potter et al., 1996;Bouwman et al., 2005a;Mayorga et al., 2010;Howarth et al., 1996). Thus we focus on N inputs that occur via deposition and fixation and losses from soil along gaseous (ammonia-volatilization,

nitrification, denitrification) ($f_{gas\ all}$) and leaching pathways ($f_{leaching}$). Hence we derive the following set of equations:

$$\delta^{15}N_{soil} = \delta^{15}N_I + \varepsilon_{gas\_all} \times f_{gas\_all} + \varepsilon_L \times f_{leaching} \quad (2)$$

$$f_{gas\_all} + f_{leaching} = 1 \quad (3)$$

where $\delta^{15}N_{soil}$ is the isotopic composition of bulk soil; $\delta^{15}N_I$ is that of atmospheric inputs; and ε_L and ε_{gas_all} is the enrichment factor for leaching and gaseous losses, respectively [ε (‰) = ($^{14}k/^{15}k - 1$) · 1000], where *k* is a rate constant

Gaseous loss pathways include nitrification/denitrification processes and ammonia volatilization. In our model, denitrification includes both denitrification and nitrifier-denitrification, since these bacterial-groups fractionate N isotopes similarly (Sutka *et al.*, 2006). From this point forward, "N gas" refers to collective denitrification; we account for the magnitude and isotopic impact of ammonia volatilization using results from previous models. We further partitioned $f_{gas\ all}$ to f_{gas} and f_{NH3}:

$$\varepsilon_{gas\_all} \times f_{gas\_all} = \varepsilon_G \times f_{gas} + \varepsilon_{NH3} \times f_{NH3} \quad (4)$$

$$f_{gas} + f_{NH3} = f_{gas\_all} \quad (5)$$

From (2), (3), (4), and (5) one gets:

$$f_{gas} = \frac{\delta^{15}N_{soil} - \delta^{15}N_I - (\varepsilon_{NH3} - \varepsilon_L) \times f_{NH3} - \varepsilon_L}{\varepsilon_G - \varepsilon_L} \quad (6)$$

The N inputs to natural ecosystems via fixation and deposition have relatively low $^{15}N/^{14}N$ ratios that do not appear to vary substantially from system to system. N_2 fixation, for example, does not appear to fractionate N_2 in air; its $\delta^{15}N$ is close to 0‰ (Boddey et

148 al., 2000;Yoneyama et al., 1986;Shearer and Kohl, 1986). In addition, the isotopic
149 composition of deposited N is typically in the range of -3‰ to 3‰ (Buzek et al.,
150 1998;Handley et al., 1999;Freyer et al., 1996;Houlton et al., 2006), with bulk nitrate
151 deposition across various latitudes, altitudes, climates and biomes averaging $\delta^{15}N$ of -
152 1.5‰ (Houlton and Bai, 2009). While ammonium and dissolved organic N compounds
153 can also be deposited, their $^{15}N/^{14}N$ ratios either overlap with or are somewhat ^{15}N-
154 depleted relative to that of nitrate in bulk precipitation (Cornell et al., 1995;Heaton et al.,
155 1997;Houlton et al., 2006). Combining both fixation and deposition inputs, $\delta^{15}N_I$ is thus
156 in the range of -1.5‰ to 0‰, in accord with previous syntheses (i.e., -2‰ to 1‰,
157 (Handley *et al.*, 1999)). We do not consider rock N inputs, though this may be an
158 important term for future N isotopic modeling efforts (Morford et al., 2011).

159 Although N leaching pathways could remove low $\delta^{15}N$ compounds from soil (ε_L)
160 in principle, empirical data suggest that the discrimination is small. *Shi* (1992) found the
161 fractionation factor of losses by dissolved NH_4^+-N was 0‰ to 0.5‰. Feuerstein et
162 al.(1997) reported that $\delta^{15}N$ of DON was 1-2‰ lower than coexisting particulate organic
163 matter in surface water of the Great Lakes. Densmore et al.(2000) noted the difference
164 between $\delta^{15}N$ of soil total N and $\delta^{15}N$ of leachable N was within 1‰ at Irwine and
165 Bicycle basins in California. Houlton et al.(2006) found that the difference between the
166 $\delta^{15}N$ stream total dissolved N and soil total N was no more than 1-2‰ across a suite of
167 Hawaiian forests. Finally, Houlton and Bai (2009) found that the $\delta^{15}N$ of nitrate in small
168 drainage streams was very close to that of soil particulate matter from arctic to tropical
169 biomes, with an integrated ε_L equal to 0.85‰. This latter analysis pointed to uniformly
170 small isotope effect expression of nitrification at the scale of entire ecosystems. Thus, we

171 use a ^{15}N discrimination of 1‰ for ε_L in our model parameterization scheme, and 0‰ -
172 5‰ in our model uncertainty analysis (see below).

173 Gaseous N losses substantially discriminate against ^{15}N along three major paths –
174 denitrification, nitrification, and ammonia volatilization. Isotope fractionation during
175 ammonia volatilization is high (ε_{NH3}, 29‰ based on (Hogberg, 1997)), and has been
176 shown to elevate the $\delta^{15}N$ of heavily grazed terrestrial ecosystems; however, ammonia
177 volatilization from soils under natural vegetation accounts for a small fraction of N losses,
178 less than 5% of total gaseous losses (Bouwman *et al.*, 1997). Consequently, this process
179 plays a minor role in elevating $\delta^{15}N_{soil}$ globally. By contrast, bacterial pathways of
180 gaseous N removal lead to significant ^{15}N enrichments – and with a flux that is large
181 enough to substantially elevate the $\delta^{15}N$ of soil above atmospheric N inputs. Indeed, the
182 average isotope effect of denitrification on nitrate is substantial in both pure culture (~
183 20‰) (Wellman *et al.*, 1968) and in natural soil communities (~ 16‰) (Houlton and Bai,
184 2009). Consistent with empirical studies, we assume that nitrifier and denitrifier gases
185 impart similar fractionations of N isotopes (Yoshida, 1988;Jinuntuya-Nortman et al.,
186 2008), and we use a combined enrichment factor (ε_G) to represent the isotope effect of
187 both processes on terrestrial $^{15}N/^{14}N$. We use an ε_G of 16 ‰ in our model
188 parameterization, allowing it to vary between 16‰ - 20‰ in our model uncertainty
189 analysis (see below). We did not account for further (i.e., values below 16 ‰) isotopic
190 underexpression of denitrification, as this seems to be an important factor at very high
191 rainfall levels (e.g., MAP > 4 m), regimes which constitute a very small (<1%) area of
192 global land environment (Bai and Houlton, 2009).

Finally, geographic distributions of $\delta^{15}N_{soil}$ are relatively well known, with many compilations pointing to similar patterns across Earth's major ecosystems (Amundson et al., 2003;Handley et al., 1999;Martinelli et al., 1999). To estimate $\delta^{15}N$ at the scale of regions and biomes, we use the large-scale (i.e., regions, biomes) assessment in ref. (Amundson *et al.*, 2003), which is based on empirical modelling. The range of $\delta^{15}N_{soil}$ globally is -2.1‰ to 10.4‰, generally higher than $\delta^{15}N_I$, indicating that $\delta^{15}N_{soil}$ is elevated compared to external N inputs. The standard variation of the estimate is 2.11 and the uncertainty is 40.7%. Although this approach may introduce errors at small scales, it reasonably approximates shifts in $\delta^{15}N$ across temperate vs. tropical biomes to within ~ 1 or 2 ‰ of empirical observations (Houlton and Bai, 2009). Thus, we use this model to integrate soil $\delta^{15}N$ across ecosystems, realizing that it may slightly underestimate the actual magnitude of terrestrial ^{15}N enrichment, pointing to the conservative nature of our isotopic approach overall. It should be noticed that above equations represent long-term equilibrium values rather than short-term (< decade) responses and our model is the integration of all isotopic-fractionating emissions over the course of ecosystem development (a few decades to centuries).

2.2 N deposition and N fixation

When the isotope model is coupled with N input models, f_{gas} can be converted to fluxes at steady state:

$$N_{gas} = (N_{fixation} + N_{deposition}) \times f_{gas} \quad (7)$$

Global symbiotic N_2 fixation (1 X 1 degree) is generated from the CASACNP model (Wang et al., 2007;Houlton et al., 2008;Wang and Houlton, 2009;Wang et al., 2010). Asymbiotic N_2 fixation is based on the biome average reported in (Cleveland *et*

al., 1999) and the global biome classification in CASACNP (Wang et al., 2007;Wang et al., 2010). Global N deposition (5 degree × 3.75 degree) is generated from a three dimensional chemistry-transport model run in the early 1990s (Lelieveld and Dentener, 2000). The total global N input to natural ecosystems is equal to 129 Tg N yr^{-1} in our model analysis. Global ammonia volatilization fluxes for natural soils are based on the biome averages as reported in (Bouwman *et al.*, 1997).

2.3 N gas production submodel

We use an index of water filled pore space (WFPS, %) to represent the "holes" in the conceptual N flux pipe (Davidson, 1991), simulating the effects of O_2 availability on gaseous N emissions. Nitrification and nitrifier-denitrification are the main N gas producing processes when WFPS is low and denitrification increases in importance when WPFS is more than 60% (Bateman and Baggs, 2005). When WFPS exceeds 80%, N_2 becomes the major gaseous N form (Davidson, 1991). Based on empirical findings (Bateman and Baggs, 2005) and previous modelling of the relationship between WFPS of soil and relative fluxes of N gases (Davidson, 1991;Potter et al., 1996), we use an index of WFPS to develop our "gas partitioning curve" (Fig. 3).

After (Potter *et al.*, 1996), the index of WFPS is unitless and is estimated by:

$$WFPS = (E + FC) / PS \qquad E>0 \qquad (8a)$$

$$WFPS = W / PS \qquad E=0 \qquad (8b)$$

235 Where FC is soil field capacity (m/m); PS is soil pore space capacity (m/m); W is
236 monthly mean soil water content (m/m); and E is excess moisture input (i.e. monthly
237 runoff) (m/m). Where WFPS exceeds 100%, 100% is used in the modelling.

238 We compiled observations of $N_2O/(NO+N_2O)$ and $N_2O/(N_2O+N_2)$ as a function
239 of water filled pore space (WFPS) from various lab and field studies (Supplementary
240 Table 1) in order to validate our N gas submodel (Fig. 4). Agreement between modelled
241 and observed ratios is measured using Root Mean Squared Error (RMSE):

242 $$RMSE = \sqrt{\frac{1}{N}\sum_{i=1}^{N}(M_i - O_i)^2} \quad (9)$$

243 where M_i is modelled $N_2O/(NO+N_2O)$ or $N_2O/(N_2O+N_2)$ ratio, O_i is the corresponding
244 observed ratio, and N is the total number of observations. RMSE is equal to 0.20 for
245 $N_2O/(NO+N_2O)$ ratios (n=46) and 0.42 for $N_2O/(N_2O+N_2)$ ratios (n=69). When WFPS is
246 low, NO is the major form of gaseous N loss; at higher WFPS, more N_2O is produced;
247 when WFPS >70%, due to increasing anaerobic conditions, N_2 production increases
248 rapidly and becomes the dominate form of gaseous N (Fig. 4). We used the coefficient of
249 variation (CV) of the global total denitrification flux to calculate the modelled range
250 (mean ± CV) of each gas form (see above).

251 **2.4 Seasonal variations of NO in Africa**

252 Seasonal variations of NO in Africa were estimated using our model and
253 GOMES satellite observations (Jaegle *et al.*, 2004). Mean annual total N gaseous fluxes
254 were first apportioned equally to each month, and then partitioned to NO, N_2O and N_2

255 fluxes based on monthly mean WFPS (see above). Modelled NO in Jan., Jun., and Aug.
256 (Fig. 5a) reflects the recent fifty-year-mean (1948-2008) monthly variations in WFPS.

257 **2.5 Data sets**

258 After (Amundson *et al.*, 2003), we estimate soil $\delta^{15}N$ by applying multiple
259 regression models to climate data:

260 $$\delta^{15}N_{soil} = 0.2048 \times MAT - 0.0012 \times MAP + 4.32 \quad (10)$$

261 The model is based on empirical relationships observed across various climnosequences,
262 spanning different biomes and climatic conditions. Mean annual temperature (MAT) and
263 precipitation (MAP) data (0.5 X 0.5 degree) are from ref. (Willmott and Matsuura, 2000).
264 The global unmanaged surface (0.1 X 0.1 degree) is based on the biome classification
265 scheme of VUB and VITO, derived from a full year cycle (1998-1999) of 10-daily
266 composites of SPOT-VEGETATION (www.geosuccess.net/Geosuccess). Areas
267 classified as croplands, urban and built-up, and cropland and natural vegetation mosaic
268 are considered as human-managed.

269 Soil moisture and runoff data are from ref. (Fan and van den Dool, 2004),
270 available on a 0.5° × 0.5° monthly basis for year1948 to the present, based on a one-layer
271 "tipping-bucket" model (Mintz and Serafini, 1981;Huang et al., 1996) that uses the
272 spatially explicit estimates of soil properties based on IGBP soil texture attributes.
273 Global soil field capacity (FC) and soil texture data are from (Webb *et al.*, 2000) (1 X 1
274 degree). Soil pore space capacity (PS) is computed from IGBP soil texture (see eqn. 7 in
275 (Saxton *et al.*, 1986)).

276 **2.6 Sensitivity and uncertainty analyses**

277 Sensitivity analyses are conducted by evaluating the response in global
278 denitrification fluxes resulting from changes in model input parameters at a level of ±
279 10 %. Results of this analysis indicate a sensitivity range from 1.3 to 11.9% (Fig. 6).
280 Global denitrification is most sensitive to soil $\delta^{15}N$ ($\delta^{15}N_{soil}$) and the effective isotope
281 effect of denitrification (ε_G): a +10% increase in either $\delta^{15}N_{soil}$ or ε_G results in +11.9% or
282 -11.9% variation in denitrification, respectively. A 10 % increase in the N input flux
283 (N_{input}) corresponds to a 10 % increase in N outputs as implied by our steady state
284 assumption. Therefore, additional constraints on $\delta^{15}N_{soil}$ and ε_G would most improve the
285 model's accuracy.

286 We used Monte Carlo methodology to estimate uncertainties in global
287 denitrification. Assuming that the errors in $\delta^{15}N_{soil}$, $\delta^{15}N_i$, f_{NH3}, and N_{input} are normal
288 distributed with a coefficient of variation of 50%, and the errors of N isotope enrichment
289 factors are uniformly distributed within the range of 25‰ - 35‰ for ε_{NH3}, 16‰ - 20‰
290 for ε_G, and 0‰ - 5‰ for ε_L, we randomly sampled 10000 sets of these seven parameters
291 from the prescribed probability distributions to estimate the mean and uncertainty of
292 denitrification for each grid cell at 0.5° × 0.5° resolution.

293 The mean global denitrification rate (μ_T) was calculated as the sum of the means
294 of all grid cells. For the uncertainty, we considered spatial correlations of errors among
295 adjacent grid cells. We first performed variogram analysis (Isaaks and Srivastava, 1989),
296 which indicated that gaseous emissions were correlated within a range distance of 84
297 cells (c. 4662 km). Based on this correlogram, we then estimated a correlation
298 coefficient between two grid cells (cell (i, j) and cell (k, l)) ($\rho_{ij,kl}$):

299 $$\rho_{ij,kl} = 1 - \frac{\gamma(h)}{VAR} \quad (11)$$

300 where γ(h) is the semi-variogram of the two grid cells with a distance of h, VAR is the
301 total variance of all grid cells. We used an exponential model to describe the variation of
302 γ(h) with *h*. That is:

303 $$\gamma(h) = Co + Cs \times (1 - e^{-(3h/a)}) \quad (12)$$

304 where C_0 is the nugget (=0.10 for our data), C_s is the partial sill (=0.36 for our data), and
305 a is the range (=42 decimal degree for our data) of the variogram model.

306 The standard deviation of the mean global denitrification rate (i.e., σ_T) was
307 calculated as:

308 $$\sigma^2{}_T = \sum_{i=1}^{N}\sum_{j=1}^{M}\sum_{k=1}^{N}\sum_{l=1}^{M}\sigma_{ij} \times \sigma_{kl} \times \rho_{ij,kl} \quad (13)$$

309 where i, k and j, l refer to row and column numbers of the global grid cells; N and M
310 refer to total latitudinal and longitudinal cells, respectively.

311 The uncertainty in the global denitrification rate is expressed as the coefficient of
312 variation (i.e. σ_T/ μ_T) and the range is expressed at the 68 % confidence interval (i.e. [μ_T-
313 σ_T, $\mu_T+\sigma_T$]).

314 **3. Results**

315 3.1 **N loss pathways**

316 At the global scale, our model indicates that 35% of all N inputs to the natural
317 land biosphere is lost to denitrification each year. This agrees with results from (Houlton
318 and Bai, 2009), in which the N isotope composition of the entire natural land biosphere
319 suggested that about 1/3 of total N inputs are lost back to the atmosphere via soil
320 denitrification pathways. It is also reasonably consistent (Seitzinger et al., 2006)
321 estimate of 44 %, which is based on numerical simulation models. Thus, our spatially-
322 explicit analysis using N stable isotope constraints on the global N budget point to a
323 substantial role for denitrification gases in removing N from land ecosystems, helping to
324 close the overall global N budget.

325 Perhaps more important, across the terrestrial biosphere, f_{gas} varies substantially.
326 Specifically, our analysis suggests that gaseous N losses vary from 0% to 69% of total N
327 inputs across temperate vs. tropical latitudes (Fig. 7a). The highest gas loss fractions are
328 associated with desert sites, where precipitation << potential evaportranspiration and
329 hydrologic leaching is minimal. Although the absolute fluxes in these areas may be low
330 due to low N inputs, gaseous N efflux is estimated to be high relative to leaching,
331 consistent with previous analyses (Galbally et al., 2008;Hartley and Schlesinger, 2000).
332 In contrast, f_{gas} decreases at higher latitudes, where limited quantities of nitrate, low NPP,
333 and low temperatures (T) constrain denitrification for most of the year. In these
334 environments, leaching ($f_{leaching}$) is the dominate vector of N loss. Globally, we estimate
335 that 65% of total N losses occurs via leaching, consistent with previous estimates (i.e.,
336 72%) for natural terrestrial ecosystems (Bouwman et al., 2005b).

337 Our results also point to marked spatial clustering in the magnitude of
338 denitrification within the natural terrestrial biosphere, with a global denitrification flux

339 equal to 46.9 ± 13.6 Tg N yr^{-1}, within the range of previous estimates (58 Tg N yr^{-1})
340 (Seitzinger *et al.*, 2006). The highest fluxes are inferred for central Africa, South
341 America, and Southeast Asia, where the combination of warm temperatures, moist soil
342 conditions, and high N availability favors high rates of soil microbial activity (Fig. 7b).
343 This agrees with previous work pointing to high potential for denitrification in moist
344 tropical sites (Potter et al., 1996;Galloway et al., 2004). Monte Carlo analysis reveals a
345 coefficient of variation (CV) of 29% on our estimates for global denitrification fluxes.

346 In terms of dissolved pathways of N loss, we estimate that 85.7 ± 24.8 Tg of
347 dissolved N compounds leach through the plant rooting zone annually. Southern United
348 States, northern South America, central Africa, and southern Asia display the largest
349 leaching fluxes due to a combination of high N inputs and high precipitation amounts
350 (Fig. 7c). Below the plant rooting zone (0-50 cm), leached N (especially nitrate) may be
351 further denitrified as it enters ground water and streams (Seitzinger *et al.*, 2006). While
352 the fate of this N is beyond the scope of this study, our results provide an independent
353 estimate of dissolved N losses that can be incorporated into future studies of
354 denitrification along the soil-river continuum. For example, our modelled spatial pattern
355 of N leaching is similar to that of DIN yield predicted by NEWS-DIN (Dumont *et al.*,
356 2005). Further, leaching is important beyond its role as a vehicle of N removal from the
357 land: it strongly influences the productivity of the coastal ecosystems and contributes to
358 coastal hypoxia and anoxia.

359 **3.2 Gaseous N forms**

360 Our model integrates multiple datasets and several submodels, which is common for
361 global-scale biogeochemical cycles due to large spatial and temporal integration (Charria
362 et al., 2008;Schaldac and Pries, 2008;Thornton et al., 2009). Uncertainty in our model
363 includes both model assumptions and model input parameters. In particular, we assume
364 ecosystem isotope balance, whereby internal N cycling processes – plant uptake,
365 microbial uptake – do not influence bulk soil $^{15}N/^{14}N$ ratios (Amundson et al.,
366 2003;Houlton et al., 2006;Bai and Houlton, 2009). This assumption seems to be valid at
367 the scale of decades to centuries for most natural sites (Amundson *et al.*, 2003); modern
368 rates of N accumulation would have at most changed soil N pools <0.1% over the past
369 100 years, implying negligible N accumulation effects on our isotopic calculations
370 (Houlton and Bai, 2009). The steady-state assumption may be less valid in sites where
371 relatively frequent and hot fires can lead to transient imbalances in N – especially on
372 short time scales (Aranibar *et al.*, 2003) (see below on importance of fire in N losses).
373 Moreover, we use an empirically-derived model to estimate soil $\delta^{15}N$ across global
374 ecosystems and this imparts errors in our assessment of $\delta^{15}N$, especially at sub-grid scales.
375 This is an important area for future work – more data on the $\delta^{15}N$ of soil across
376 ecosystems. Nevertheless, we note that the approach we used to estimate soil $\delta^{15}N$ is able
377 to capture shifts across temperate to tropical biomes, typically within about 1‰ of actual
378 measurements (Houlton and Bai, 2009).

379 We estimate that, on average, 0.152 ± 0.044 g N m^{-2} yr^{-1} are lost to microbial NO
380 production in the natural terrestrial soil (Table 1, Fig. 8a). Globally, the geographic area
381 that is free from agriculture and major land cover transformation is equal to 103.5 10^{12} m^2
382 (based on VUB and VITO). Applying this area to our NO production rates, we calculate

383 that 11.2-20.3 Tg N yr^{-1} are emitted as NO globally. This estimate is significantly higher
384 than natural NO emissions (3-8 Tg N yr^{-1}) as summarized in the Inter-governmental
385 Panel on Climate Change's (IPCC) fourth assessment report (AR4) (Denman *et al.*, 2007).
386 Combining our estimate of natural NO emissions with that of cropland and managed
387 grassland (Stehfest and Bouwman, 2006) (i.e., 1.8 Tg N yr^{-1}), we calculate a total NO
388 flux of 13.0-22.1 Tg N yr^{-1} for the entire terrestrial biosphere (i.e., managed plus
389 unmanaged). This falls between those of most process-(Potter *et al.*, 1996) (9.7 Tg N yr^{-1})
390 and empirically-based models (Davidson and Kingerlee, 1997) (21.1 Tg N yr^{-1}) (Table 1),
391 but is higher than some estimates reported in the literature (5-8 Tg N yr^{-1}) (Yan et al.,
392 2005;Yienger and Levy, 1995;Lee et al., 1997) (Table 1).

393 Regionally, highest NO emissions are simulated for mesic to dry tropical
394 environments (Fig. 8a). Among the continents Africa emerges as the largest source for
395 NO in the natural terrestrial biosphere (0.213-0.657 g N m^{-2} yr^{-1}, Table 2). Our model
396 simulates high NO emissions in tropical savanna/woodland environments (0.267-0.711 g
397 N m^{-2} yr^{-1}, Table 2) while tundra falls at the low end of the worldwide NO spectrum (0-
398 0.007 g N m^{-2} yr^{-1}, Table 2). Nitric oxide fluxes vary from 0.023-0.055 g N m^{-2} yr^{-1} for
399 temperate forest sites, in agreement with empirical data (Supplementary Table 2). In
400 global grasslands, we estimate microbial NO emissions between 0.101-0.179 g N m^{-2} yr^{-1},
401 or near the upper bound of previously published data (Supplementary Table 2).

402 Importantly, the rate of emission of NO from the soil is higher than the flux to the
403 atmosphere, owing to scavenging of NO by canopy vegetation (Bakwin *et al.*, 1990).
404 Nitric oxide is often quickly oxidized to NO_2 upon emission, and can be absorbed onto
405 vegetation surfaces, reducing the total amount of NO_x that escapes to the atmosphere

406 (Davidson and Kingerlee, 1997). Using leaf absorption factors (Yienger and Levy, 1995),
407 we suggest that net emission of NO from unmanaged terrestrial ecosystems may be
408 reduced by up to 10 Tg N yr^{-1}. Comparing our modelled spatial and temporal variations
409 of soil surface NO emissions to satellite mapping of space-based observation of NO_2 in
410 Africa (Jaegle *et al.*, 2004) (Fig. 5), we find that both soil microbial activities and fire
411 activity are responsible for the high levels of atmospheric NO_2 between 0˚ to 10˚ N
412 latitude in January. In contrast, the unexpectedly high level of NO_2 above the Sahel
413 region during June (shown in the pink rectangular in Fig. 5) is not caused by fire or
414 industrial emissions; rather, Jaegle et al.(2004) speculated that this represented microbial
415 NO_x pulses following the onset of rainfall over vast areas of dry soil, a notion confirmed
416 by our model simulations (Fig. 5a). Thus, our isotope-based approach appears to integrate
417 broad-scale dynamism in microbial gaseous N production rates.

418 For N_2O, we estimate that 7.2-13.2 Tg N yr^{-1} of this potent greenhouse gas are
419 emitted from soil microbes worldwide (Table 1, Fig. 8b). Bouwman et al.(1995)
420 estimated 6.8 Tg N yr^{-1} global pre-agricultural N_2O emissions based on a simple
421 empirical model, while the IPCC adopted value of 3.3-9.9 Tg N yr^{-1} N_2O emissions from
422 soils under natural vegetations in their 2001 report (Ehhalt *et al.*, 2001). When our
423 results are combined with the N_2O efflux associated with fertilized cropland and managed
424 grassland (4.1 Tg N yr^{-1}) (Stehfest and Bouwman, 2006), we estimate a natural soil
425 sourced global N_2O flux between 11.3-17.3 Tg N yr^{-1}. Diverse global estimates of N_2O
426 are available via process-based, statistical, or inverse models; they (Huang et al.,
427 2008;Nevison et al., 1996;Ehhalt et al., 2001;Bouwman et al., 1995;Xu et al., 2008;Dalal
428 and Allen, 2008;Bowden, 1986;Potter et al., 1996;Liu, 1996;Hirsch et al., 2006) generally

429 vary from 10.6 Tg N yr^{-1} to 15 Tg N yr^{-1} (Table 1). Our isotope-based model
430 independently confirms this range of estimates of global N_2O fluxes from natural soils.

431 Across the terrestrial biosphere, our model identifies moist tropical areas, such as
432 the east Amazon basin, central Africa, and northern Australia as natural hotspots of
433 bacterial N_2O production (Fig. 8b). Specifically, we estimate that natural tropical
434 rainforest and savanna biomes account for 77 % of global natural N_2O emissions.
435 Tropical rainforests have the highest potential for N_2O production (0.176-0.400 g N m^{-2}
436 yr^{-1}, Table 2), whereas, similar to NO, tundra has the lowest (0-0.007 g N m^{-2} yr^{-1}, Table
437 2). Previous models have reported a mean range of 0.12-0.29 g N m^{-2} yr^{-1} for N_2O
438 emissions from tropical forests (Matson and Vitousek, 1990;Bowden, 1986;Dalal and
439 Allen, 2008;Potter et al., 1996) and a mean range of 0.022-0.068 g N m^{-2} yr^{-1} N_2O
440 emissions from temperate forests (Dalal and Allen, 2008;Stehfest and Bouwman, 2006).
441 Our results fall within this range – except for tropical savanna where we estimate higher
442 N_2O fluxes (0.150-0.398 g N m^{-2} yr^{-1}) than empirical- (Dalal and Allen, 2008) and
443 process-based (Potter *et al.*, 1996) models. Our model may overestimate this flux
444 because fire-caused N losses are not considered. For example, Olivier et al. (1998)
445 estimated that 4.8 Tg N yr^{-1} is removed by savanna fires, or approximately 62 % of total
446 fire-induced N gas emissions in the terrestrial biosphere. Globally, fire removes a modest
447 amount of N (7.7 Tg N yr^{-1}), ~ 5.8 % of total N inputs (Olivier *et al.*, 1998).

448 Finally, to our knowledge, we here provide the first-ever simulations of the global
449 spatial pattern of soil N_2 emissions, widely believed to be the dominant biogenic form of
450 gaseous N on Earth. We estimate that 14.9-27.1 Tg N yr^{-1} are denitrified to atmospheric
451 N_2 in the natural soil. According to our model, soil N_2 originates mainly in southeast

452 North America, north South America, central Africa, and Southeast Asia (Fig. 8c);
453 anaerobic environments caused by high precipitation and poor soil drainage in these areas
454 favor N_2 production (Galloway *et al.*, 2004). In contrast, dry and low N throughput
455 environments have uniformly low N_2 production potentials (Fig. 8c).

456 Due to methodological limitations, very few studies have assessed soil N_2 fluxes
457 in the field. Recently, Schlesinger (2009) compiled all of the available data on N_2O-
458 $N/(N_2O + N_2)$-N reported for terrestrial ecosystems under natural vegetation, with a mean
459 fraction of 0.51 for grassland (n=4), 0.41 for forest (n=14), and 1.0 for desert (n=1). Our
460 model simulates an N_2O-$N/(N_2O + N_2)$-N ratio of 0.22 for tropical and temperate forest,
461 0.43 for tropical savanna/woodland, 0.57 for grassland, and 0.71 for desert biomes – all
462 of which fit generally with Schlesinger's compilation (Schlesinger, 2009). In moist
463 tropical forest, the high water availability and periods of extended anaerobiosis in soil,
464 and high NPP and N cycling rates, favor low N_2O-$N/(N_2O + N_2)$-N ratios. In temperate
465 forests, N_2O-$N/(N_2O + N_2)$-N ratios are generally low and extremely variable. For
466 example, Wolf and Brumme (2003) reported N_2O-$N/(N_2O + N_2)$-N ratios ranging
467 between 0.19 to 0.85 in beech forest with different mineral soils; Merrill and Zak (1992)
468 found a much higher values (0.63-0.98) in upland forest in Michigan and a N_2O-$N/(N_2O$
469 $+ N_2)$-N ratio of 0.25 under swampy forest conditions. Dannenmann et al.(2008)
470 observed a N_2O-$N/(N_2O + N_2)$-N ratio of 0.23 when water holding capacity (WHC) was
471 48-55%, while the ratio dropped to 0.03 when WHC was 62-84%.

472 **4. Discussion**

Our results point to tropical ecosystems as the global N cycling hotspot within the natural land surface. This agrees with field-based evidence (Vitousek, 1984;Hedin et al., 2009), and implies a potential coupling between natural paths of fixation (Houlton *et al.*, 2008) and denitrification within this biome, similar to those couplings observed for the global open ocean (Deutsch *et al.*, 2007). Future studies on N_2 fixation and denitrification (and their couplings) in tropical forests are critical for understanding the integrated Earth-climate system – and the magnitude and direction of carbon (C) exchanges between tropical biomes and the atmosphere.

Accurate partitioning of N losses along denitrification vs. leaching vectors is fundamental to understanding C and N couplings in the terrestrial biosphere. The response of N-limited ecosystem to increasing [CO_2] depends partly on N loss responses to increasing [CO_2] in the future. Losses of DON compounds are substrate-independent (Hedin *et al.*, 2003) and therefore less likely to change with increasing [CO_2] (Rastetter *et al.*, 2005) than are N losses via nitrate leaching and denitrification that depends on available N substrates; denitrification in particular might be expected to decrease in response to progressive N-limitation. Our study reveals that leaching is a greater fraction of N losses (~77%) at high latitudes, in contrast to the tropics where denitrification (leaching = 58%) contributes more to the N economy of ecosystems. These results agree with empirical studies pointing to substantial DON losses from both boreal and unpolluted temperate forests and high denitrification rates in tropical sites (Seitzinger et al., 2006;Neff et al., 2003). We postulate that loss-driven N limitation will persist longer at high latitudes than other sectors of the terrestrial biosphere.

Global biogeochemical models have been used to study the change of nutrient limitation under future climate and higher [CO_2] conditions (Sokolov et al., 2008;Thornton et al., 2009;Zaehle et al., 2010a); but the spatial pattern of N limitation and its response to increased warming and [CO_2] is uncertain. For example, N limitation of tropical NPP is expected in one model (Thornton et al., 2009), whereas another model suggests that temperate and boreal forests will exhibit more profound symptoms of progressive N limitation than tropical forests in the future (Zaehle *et al.*, 2010b). Global models of C and N cycles are poorly constrained (Wang et al., 2010); uncertainties in their predictions are expected to be high, but yet to be quantified. The spatially explicit estimates of N losses from this study can provide an important constraint for benchmarking the performance of global biogeochemical models under present conditions. Additional work on the N isotope composition of natural ecosystems, coupled with examination for transient effects where appropriate, would not only advance our approach further, but would also be useful for ground-truthing global models.

Our isotope-based approach considers interactions between soil microbial processes, climate and soil conditions over large spatial scales thereby providing a novel and independent constraint against which empirical- and process-based models and inverse chemical transport analyses can be evaluated. Our isotope-based approach points to high NO emissions in Africa and high N_2 emissions in Southeast USA, areas where very few measurements have been made. Incorporating spatial and temporal complexities (so-called "hotspots and hot moments") into the N cycle is considered the biggest challenge in denitrification research (Groffman *et al.*, 2009). Previous studies have used models that were calibrated locally and extrapolated globally, introducing

518 unquantifiable uncertainties into estimates of denitrification. Episodic emissions of NO
519 and N_2O in the arid and semiarid region are known to account for a significant fraction of
520 total N loss (Hartley and Schlesinger, 2000), for example, and these losses are poorly
521 simulated by most global models, whereas our model integrates all isotopic-fractionating
522 emissions including episodic pulses of NO and N_2O over a long period (> decade). The
523 similarities between our modelled results and satellite observations of NO_2 and newly
524 identified hot spots of N emissions points to the power of our N isotope model at large
525 scales.

526 Our modelled maps provide a reference for future studies. For example, our map
527 (Fig. 8b) points to the Congo Basin in Africa as one of the dominant natural sources of
528 N_2O– a potent greenhouse gas (Fig. 1) and ozone-depleting agent (Ravishankara *et al.*,
529 2009) – while there are almost no published data on N_2O fluxes from this region. Most
530 published data on N_2O fluxes in the tropics are from South and Central American forests,
531 with a few data from Southeast Asia and Northwest Australia. Thus continued
532 advancement on such issues as climate change and stratospheric ozone would seem to
533 benefit from empirical investigations of the old-world tropics.

534 The spatial patterns of N_2 emissions we describe are crucial for understanding N
535 dynamics of the Earth system. Soil N_2 is considered the most important pathway by
536 which N is returned from the soil to the atmosphere (Schlesinger, 2009;Galloway et al.,
537 2004). . Our results support the common belief that N_2 emissions account for a
538 significant fraction of the "missing N" (Schlesinger, 2009) in the global N cycle and
539 provide the first-ever quantitative predictions of global patterns of N_2 fluxes among
540 terrestrial ecosystems.

Our model can be improved with additional information, observations and experiments. In particular, knowledge on isotope fractionations via gaseous N losses are clearly warranted, since they can vary across different ecosystems and conditions; our sensitivity analyses (Fig. 6) indicate that our N loss fractions are most sensitive to variation in $\delta^{15}N$ ($\delta^{15}N_{soil}$) and the isotope effect of denitrification (ε_{den}). This points to the importance of a deeper understanding of isotope effect expression and additional measurements of soil $\delta^{15}N$. In addition, more information on the influence of soil properties such as soil texture, soil water availability on N gas partitioning would increase the robustness of our model. Further, uncertainties in N_2 fixation models are difficult to assess and are probably high, although they are the best available models at present; additional constraints on N inputs and climate and soil databases could help to reduce uncertainties in the model.

Finally, our estimates of N loss fractions have implications for a rapidly changing N cycle. Nitrogen deposition is on the rise and will continue to rise into the future, spreading rapidly into tropical ecosystems globally (Galloway et al. 2008). Our results suggest that N inputs into tropical environments and arid sites will disproportionately mobilize to atmospheric gases when compared to extra-tropical moist environments, particularly boreal and temperate forests. Rising levels of N deposition to tropical ecosystems could release more N_2O from soils to the atmosphere (see also (Matson et al., 1999)), warming the climate in a way that is fundamentally different than what has already been observed for N deposition effects at the higher latitudes..

Acknowledgements

563 Funded by the Andrew W. Mellon Foundation, financial support from Key Program of
564 the Chinese Academy of Sciences Project KZCX2-YW-BR-20 to EB, and
565 Department of Climate Change, Australia to YPW.

566 **References**

567 Altabet, M. A., Francois, R., Murray, D. W., and Prell, W. L.: Climate-related
568 variations in denitrification in the Arabian Sea from sediment $^{15}N/^{14}N$ ratios, Nature, 373,
569 506-509, 1995.

570 Amundson, R., and Baisden, W. T.: Stable isotope tracers and models in soil
571 organic matter studies, in: Methods in Ecosystem Science, edited by: Sala, O., Mooney,
572 H., Howarth, B., and Jackson, R. B., Springer Verlag, New York, NY, 117-137, 2000.

573 Amundson, R., Austin, A. T., Schuur, E. A. G., Yoo, K., Matzek, V., Kendall, C.,
574 Uebersax, A., Brenner, D., and Baisden, W. T.: Global patterns of the isotopic
575 composition of soil and plant nitrogen, Global Biogeochemical Cycles, 17, 1031,
576 10.1029/2002GB001903, 2003.

577 Aranibar, J. N., Macko, S. A., Anderson, I. C., Potgieter, A. L. F., Sowry, R., and
578 Shugart, H. H.: Nutrient cycling responses to fire frequency in the Kruger National Park
579 (South Africa) as indicated by stable isotope analysis, Isotopes in Environmental Health
580 Studies, 39, 141-158, 2003.

581 Bai, E., and Houlton, B. Z.: Coupled isotopic and process-based modeling of
582 gaseous nitrogen losses from tropical rain forests, Global Biogeochemical Cycles, 23,
583 doi:10.1029/2008GB003361, 2009.

584 Bakwin, P. S., Wofsy, S. C., Fan, S.-M., Keller, M., Trumbore, S. E., and Da Costa,
585 J. M.: Emission of nitric oxide (NO) from tropical forest soils and exchange of NO

586 between the forest canopy and atmospheric boundary layers, J. Geophys. Res., 95,
587 16755–16764, 1990.
588 Bateman, E. J., and Baggs, E. M.: Contributions of nitrification and denitrification
589 to N_2O emissions from soils at different water-filled pore space, Biol. Fertil. Soils, 41,
590 379-388, 2005.
591 Boddey, R. M., Peoples, M. B., Palmer, B., and Dart, P. J.: Use of the ^{15}N natural
592 abundance technique to quantify biological nitrogen fixation by woody perennials, Nutr.
593 Cycl. Agroecosyst., 57, 235-270, 2000.
594 Bouwman, A. F., Van der Hoek, K. W., and Olivier, J. G. J.: Uncertainties in the
595 global source distribution of nitrous oxide, J. Geophys. Res., 100, 2785–2800, 1995.
596 Bouwman, A. F., Lee, D. S., Asman, W. A. H., Dentener, F. J., Van Der Hoek, K.
597 W., and Olivier, J. G. J.: A global high-resolution emission inventory for ammonia,
598 Global Biogeochemical Cycles, 11, 561-587, 1997.
599 Bouwman, A. F., Deecht, G. V., and Hoek, K. W. V. d.: Global and regional
600 surface nitrogen balances in intensive agricultural production eystems for the period
601 1970-2030, Pedosphere, 15, 19, 2005a.
602 Bouwman, A. F., Van Drecht, G., Knoop, J. M., Beusen, A. H. W., and Meinardi, C.
603 R.: Exploring changes in river nitrogen export to the world's oceans, Global
604 biogeochemical cycles, 19, doi:10.1029/2004GB002314, 10.1029/2004gb002314, 2005b.
605 Bowden, W.: Gaseous nitrogen emissions from undisturbed terrestrial ecosystems:
606 an assessment of their impacts on local and global nitrogen budgets, Biogeochemistry, 2,
607 249-279, 1986.

608 Boyer, E. W., Alexander, R. B., Parton, W. J., Li, C., Butterbach-Bahl, K., Donner,
609 S. D., Skaggs, R. W., and Del Grosso, S. J.: Modeling denitrification in terrestrial and
610 aquatic ecosystems at regional scales, Ecol. Appl., 16, 2123-2142, 2006.
611 Brenner, D. L., Amundson, R., Baisden, W. T., Kendall, C., and Harden, J.: Soil N
612 and ^{15}N variation with time in a California annual grassland ecosystem, Geochim.
613 Cosmochim. Acta, 65, 4171-4186, 2001.
614 Butterbach-Bahl, K., Willibald, G., and Papen, H.: Soil core method for direct
615 simultaneous determination of N_2 and N_2O emissions from forest soils, Plant Soil, 240,
616 105-116, 2002.
617 Buzek, F., ern, yacute, J, and Paes, T.: The behavior of nitrogen isotopes in
618 acidified forest soils in the Czech Republic, Water, Air, and Soil Pollution, 105, 155-164,
619 1998.
620 Charria, G., Dadou, I., Llido, J., Drévillon, M., and Garçon, V.: Importance of
621 dissolved organic nitrogen in the north Atlantic Ocean in sustaining primary production:
622 a 3-D modelling approach, Biogeosciences, 5, 1437-1455, 2008.
623 Cleveland, C. C., Townsend, A. R., Schimel, D. S., Fisher, H., Howarth, R. W.,
624 Hedin, L. O., Perakis, S. S., Latty, E. F., Von Fischer, J. C., Elseroad, A., and Wasson, M.
625 F.: Global patterns of terrestrial biological nitrogen (N_2) fixation in natural ecosystems,
626 Global Biogeochemical Cycles, 13, 623–645, 1999.
627 Cornell, S., Rendell, A., and Jickells, T.: Atmospheric inputs of dissolved organic
628 nitrogen to the oceans, Nature, 376, 243-246, 1995.
629 Craine, J. M., Elmore, A. J., Aidar, M. P. M., Bustamante, M., Dawson, T. E.,
630 Hobbie, E. A., Kahmen, A., Mack, M. C., McLauchlan, K. K., Michelsen, A., Nardoto, G.

631 B., Pardo, L. H., Penuelas, J., Reich, P. B., Schuur, E. A. G., Stock, W. D., Templer, P.
632 H., Virginia, R. A., Welker, J. M., and Wright, I. J.: Global patterns of foliar nitrogen
633 isotopes and their relationships with climate, mycorrhizal fungi, foliar nutrient
634 concentrations, and nitrogen availability, New Phytol., 183, 980-992, 2009.
635 Dalal, R. C., and Allen, D. E.: Turner Review No. 18. Greenhouse gas fluxes from
636 natural ecosystems, Aust. J. Bot., 56, 369-407, doi:10.1071/BT07128, 2008.
637 Dannenmann, M., Butterbach-Bahl, K., Gasche, R., Willibald, G., and Papen, H.:
638 Dinitrogen emissions and the N_2:N_2O emission ratio of a Rendzic Leptosol as influenced
639 by pH and forest thinning, Soil Biol. Biochem., 40, 2317-2323, 2008.
640 Davidson, E. A.: Fluxes of nitrous oxide and nitric oxide from terrestrial
641 ecosystems, in: Microbial production and consumption of greenhouse gases: methane,
642 nitrogen oxides, and halomethanes, edited by: Rogers, J. E., and Whitman, W. B.,
643 American Society for Microbiology, Washington, D.C., USA, 219-235, 1991.
644 Davidson, E. A., and Kingerlee, W.: A global inventory of nitric oxide emissions
645 from soils, Nutr. Cycl. Agroecosyst., 48, 37-50, 1997.
646 Denman, K. L., Brasseur, G., Chidthaisong, A., Ciais, P., Cox, P. M., Dickinson, R.
647 E., Hauglustaine, D., Heinze, C., Holland, E., Jacob, D., Lohmann, U., Ramachandran, S.,
648 Dias, P. L. d. S., Wofsy, S. C., and Zhang, X.: Couplings Between Changes in the
649 Climate System and Biogeochemistry, in: Climate Change 2007: The Physical Science
650 Basis. Contribution of Working Group I to the Fourth Assessment Report of the
651 Intergovernmental Panel on Climate Change, edited by: Solomon, S., Qin, D., Manning,
652 M., Chen, Z., Marquis, M., Averyt, K. B., M.Tignor, and Miller, H. L., Cambridge
653 University Press, Cambridge, UK, 500-587, 2007.

654 Densmore, J. N., and Böhlke, J. K.: Use of nitrogen isotopes to determine sources
655 of nitrate contamination in two desert basins in California, in: Interdisciplinary
656 perspectives on drinking water risk assessment and management, edited by: Reichard, E.
657 G., Hauchman, F. S., and Sancha, A. M., International Association of Hydrologic
658 Sciences Publication Santiago, Chile, 63-73, 2000.
659 Deutsch, C., Sarmiento, J. L., Sigman, D. M., Gruber, N., and Dunne, J. P.: Spatial
660 coupling of nitrogen inputs and losses in the ocean, Nature, 445, 163-167, 2007.
661 Devol, A. H., Uhlenhopp, A. G., Naqvi, S. W. A., Brandes, J. A., Jayakumar, D. A.,
662 Naik, H., Gaurin, S., Codispoti, L. A., and Yoshinari, T.: Denitrification rates and excess
663 nitrogen gas concentrations in the Arabian Sea oxygen deficient zone, Deep Sea Research
664 Part I: Oceanographic Research Papers, 53, 1533-1547, 2006.
665 Dumont, E., Harrison, J. A., Kroeze, C., Bakker, E. J., and Seitzinger, S. P.: Global
666 distribution and sources of dissolved inorganic nitrogen export to the coastal zone:
667 Results from a spatially explicit, global model, Global Biogeochemical Cycles, 19,
668 10.1029/2005gb002488, 2005.
669 Ehhalt, D., Prather, M., Dentener, F., Derwent, R., Dlugokencky, E., Holland, E.,
670 Isaksen, I., Katima, J., Kirchhoff, V., Matson, P., Midgley, P., Wang, M., Berntsen, T.,
671 Bey, I., Brasseur, G., Buja, L., Collins, W. J., Daniel, J., DeMore, W. B., Derek, N.,
672 Dickerson, R., Etheridge, D., Feichter, J., Fraser, P., Friedl, R., J. Fuglestvedt, M. G., L.
673 Grenfell, A. Grübler, N. Harris,, D. Hauglustaine, L. H., C. Jackman, D. Jacob, L. Jaeglé,
674 A. Jain, M. Kanakidou, S. Karlsdottir,, M. Ko, M. K., M. Lawrence, J.A. Logan, M.
675 Manning, D. Mauzerall, J. McConnell, L. Mickley,, S. Montzka, J. F. M., J. Olivier, K.
676 Pickering, G. Pitari, G.J. Roelofs, H. Rogers, B. Rognerud, S. Smith,, S. Solomon, J. S., P.

677 Steele, D. Stevenson, J. Sundet, A. Thompson, M. van Weele,, and R. von Kuhlmann, Y.
678 W., D. Weisenstein, T. Wigley, O. Wild, D. Wuebbles, R. Yantosca: Atmospheric
679 chemistry and greenhouse gases, in: IPCC Report 2001, edited by: Houghton, J. T., Ding,
680 Y., Griggs, D. J., Noguer, M., Linden, P. J. v. d., Dai, X., Maskell, K., and Johnson, C. A.,
681 Cambridge University Press, Cambridge, UK, 241-280, 2001.
682 Evans, R. D.: Physiological mechanisms influencing plant nitrogen isotope
683 composition, Trends Plant Sci., 6, 121-126, 2001.
684 Fan, Y., and van den Dool, H.: Climate prediction center global monthly soil
685 moisture data set at 0.5° resolution for 1948 to present, J. Geophys. Res., 109,
686 doi:10.1029/2003JD004345, 2004.
687 Feuerstein, T. P., Ostrom, P. H., and Ostrom, N. E.: Isotopic biogeochemistry of
688 dissolved organic nitrogen: A new technique and application, Organic Geochemistry, 27,
689 363-370, 1997.
690 Freyer, H. D., Kobel, K., Delmas, R. J., Kley, D., and Legrand, M. R.: First results
691 of $^{15}N/^{14}N$ ratios in nitrate from alpine and polar ice cores, Tellus B, 48, 93-105,
692 doi:10.1034/j.1600-0889.1996.00009.x, 1996.
693 Galbally, I. E., Kirstine, W. V., Meyer, C. P., and Wang, Y. P.: Soil-atmosphere
694 trace gas exchange in semiarid and arid zones, J. Environ. Qual., 37, 599-607,
695 10.2134/jeq2006.0445, 2008.
696 Galloway, J. N., Dentener, F. J., Capone, D. G., Boyer, E. W., Howarth, R. W.,
697 Seitzinger, S. P., Asner, G. P., Cleveland, C. C., Green, P. A., Holland, E. A., Karl, D. M.,
698 Michaels, A. F., Porter, J. H., Townsend, A. R., and Vöosmarty, C. J.: Nitrogen cycles:
699 past, present, and future, Biogeochemistry, 70, 153-226, 2004.

700 Groffman, P., Butterbach-Bahl, K., Fulweiler, R., Gold, A., Morse, J., Stander, E.,
701 Tague, C., Tonitto, C., and Vidon, P.: Challenges to incorporating spatially and
702 temporally explicit phenomena (hotspots and hot moments) in denitrification models,
703 Biogeochemistry, 93, 49-77, 2009.
704 Handley, L. L., Austin, A. T., Robinson, D., Scrimgeour, C. M., Raven, J. A.,
705 Heaton, T. H. E., Schmidt, S., and Stewart, G. R.: The ^{15}N natural abundance ($\delta^{15}N$) of
706 ecosystem samples reflects measures of water availability, Aust. J. Plant Physiol., 26,
707 185-199, 1999.
708 Hartley, A. E., and Schlesinger, W. H.: Environmental controls on nitric oxide
709 emission from northern Chihuahuan desert soils, Biogeochemistry, 50, 279-300, 2000.
710 Heaton, T. H. E., Spiro, B., Madeline, S., and Robertson, C.: Potential canopy
711 influences on the isotopic composition of nitrogen and sulphur in atmospheric deposition,
712 Oecologia, 109, 600-607, 1997.
713 Hedin, L. O., Vitousek, P. M., and Matson, P. A.: Nutrient losses over four million
714 years of tropical forest development, Ecology, 84, 2231-2255, 2003.
715 Hedin, L. O., Brookshire, E. N. J., Menge, D. N. L., and Barron, A.: The nitrogen
716 paradox in tropical forest ecosystems, Annual Review of Ecology, Evolution, and
717 Systematics, 40, doi:10.1146/annurev.ecolsys.37.091305.110246, 2009.
718 Hirsch, A. I., Michalak, A. M., Bruhwiler, L. M., Peters, W., Dlugokencky, E. J.,
719 and Tans, P. P.: Inverse modeling estimates of the global nitrous oxide surface flux from
720 1998-2001, Global Biogeochemical Cycles, 20, doi:10.1029/2004GB002443,
721 10.1029/2004gb002443, 2006.

722 Hobbie, J. E., and Hobbie, E. A.: ^{15}N in symbiotic fungi and plants estimates
723 nitrogen and carbon flux rates in Arctic tundra, Ecology, 87, 816-822, 2006.
724 Hogberg, P.: Tansley Review No. 95. ^{15}N natural abundance in soil-plant Systems,
725 New Phytol., 137, 179-203, 1997.
726 Houlton, B. Z., Sigman, D. M., and Hedin, L. O.: Isotopic evidence for large
727 gaseous nitrogen losses from tropical rainforests, Proceedings of the National Academy
728 of Sciences, 103, 8745-8750, 10.1073/pnas.0510185103, 2006.
729 Houlton, B. Z., Sigman, D. M., Schuur, E. A., and Hedin, L. O.: A climate-driven
730 switch in plant nitrogen acquisition within tropical forest communities, Proc. Natl. Acad.
731 Sci. U. S. A., 104, 8902 - 8906, 2007.
732 Houlton, B. Z., Wang, Y.-P., Vitousek, P. M., and Field, C. B.: A unifying
733 framework for dinitrogen fixation in the terrestrial biosphere, Nature, 454, 327-330, 2008.
734 Houlton, B. Z., and Bai, E.: Imprint of denitrifying bacteria on the global terrestrial
735 biosphere, Proceedings of the National Academy of Sciences, 106, 21713-21716, 2009.
736 Howarth, R., Billen, G., Swaney, D., Townsend, A., Jaworski, N., Lajtha, K.,
737 Downing, J., Elmgren, R., Caraco, N., Jordan, T., Berendse, F., Freney, J., Kudeyarov, V.,
738 Murdoch, P., and Zhao-Liang, Z.: Regional nitrogen budgets and riverine N & P fluxes
739 for the drainages to the North Atlantic Ocean: Natural and human influences,
740 Biogeochemistry, 35, 75-139, 1996.
741 Huang, J., Dool, H. v. d., and Georgakakos, L. P.: Analysis of model-calculated soil
742 moisture over the United States (1931-93) and application to long-range temperature
743 forecasts, Journal of Climate, 9, 1350-1362, 1996.

744 Huang, J., Golombek, A., Prinn, R., Weiss, R., Fraser, P., Simmonds, P.,
745 Dlugokencky, E. J., Hall, B., Elkins, J., Steele, P., Langenfelds, R., Krummel, P., Dutton,
746 G., and Porter, L.: Estimation of regional emissions of nitrous oxide from 1997 to 2005
747 using multinetwork measurements, a chemical transport model, and an inverse method, J.
748 Geophys. Res., 113, doi:10.1029/2007JD009381, 2008.
749 Isaaks, E. H., and Srivastava, R. M.: An introduction to applied geostatistics,
750 Oxford University Press, New York, New York, USA, 1989.
751 Jaegle, L., Martin, R. V., Chance, K., Steinberger, L., Kurosu, T. P., Jacob, D. J.,
752 Modi, A. I., YobouÃ©, V., Sigha-Nkamdjou, L., and Galy-Lacaux, C.: Satellite mapping
753 of rain-induced nitric oxide emissions from soils, J. Geophys. Res., 109,
754 doi:10.1029/2004JD004787, 2004.
755 Jinuntuya-Nortman, M., Sutka, R. L., Ostrom, P. H., Gandhi, H., and Ostrom, N. E.:
756 Isotopologue fractionation during microbial reduction of N_2O within soil mesocosms as a
757 function of water-filled pore space, Soil Biol. Biochem., 40, 2273-2280, 2008.
758 Kendall, C.: Tracing nitrogen sources and cycling in catchments, in: Isotope
759 Tracers in Catchment Hydrology, edited by: Kendall, C., and McDonnell, J., Elsevier Sci.,
760 New York, 1998.
761 Lee, D. S., Köhler, I., Grobler, E., Rohrer, F., Sausen, R., Gallardo-Klenner, L.,
762 Olivier, J. G. J., Dentener, F. J., and Bouwman, A. F.: Estimations of global NO_x
763 emissions and their uncertainties, Atmos. Environ., 31, 1735-1749, 1997.
764 Lelieveld, J., and Dentener, F. J.: What controls tropospheric ozone?, J. Geophys.
765 Res., 105, 3531-3551, 2000.

766 Li, C., Frolking, S., and Frolking, T. A.: A model of nitrous oxide evolution from
767 soil driven by rainfall events. I : Model structure and sensitivity, J. Geophys. Res., 97,
768 9759-9776, 1992.
769 Liu, Y.: Modelling the emission of nitrous oxide (N_2O) and methane (CH_4) from
770 the terrestrial biosphere to the atmosphere, PhD, MIT joint Program on the Science and
771 Policy of Global Change, Massachusetts Institute of Technology, Cambridge, 219 pp.,
772 1996.
773 Martinelli, L. A., Piccolo, M. C., Townsend, A. R., Vitousek, P. M., Cuevas, E.,
774 McDowell, W., Robertson, G. P., Santos, O. C., and Treseder, K.: Nitrogen stable
775 isotopic composition of leaves and soil: tropical versus temperate forests,
776 Biogeochemistry, 46, 45-65, 1999.
777 Matson, P. A., Vitousek, P. M., and Schimel, D. S.: Regional extrapolation of trace
778 gas flux based on soils and ecosystems, in: Exchange of Trace Gases between Terrestrial
779 Ecosystems and the Atmosphere, edited by: Andreae, M. D., and Schimel, D. S.,
780 Springer-Verlag, New York, NY, 97-108, 1989.
781 Matson, P. A., and Vitousek, P. M.: Ecosystem approach to a global nitrous oxide
782 budget, BioScience, 40, 667-672, 1990.
783 Matson, P. A., McDowell, W. H., Townsend, A. R., and Vitousek, P. M.: The
784 globalization of N deposition: ecosystem consequences in tropical environments,
785 Biogeochemistry, 46, 67-83, 1999.
786 Mayorga, E., Seitzinger, S. P., Harrison, J. A., Dumont, E., Beusen, A. H. W.,
787 Bouwman, A. F., Fekete, B. M., Kroeze, C., and Van Drecht, G.: Global nutrient export

788 from watersheds 2 (NEWS 2): Model development and implementation, Environmental
789 Modelling & Software, 25, 837-853, 2010.
790 McClain, M. E., Boyer, E. W., Dent, C. L., Gergel, S. E., Grimm, N. B., Groffman,
791 P. M., Hart, S. C., Harvey, J. W., Johnston, C. A., Mayorga, E., McDowell, W. H., and
792 Pinay, G.: Biogeochemical hot spots and hot moments at the interface of terrestrial and
793 aquatic ecosystems, Ecosystems, 6, 301-312, 2003.
794 Merrill, A. G., and Zak, D. R.: Factors controlling denitrification rates in upland
795 and swamp forests, Can. J. For. Res., 22, 1597-1604, 1992.
796 Mintz, Y., and Serafini, Y.: Global fields of soil moisture and land-surface
797 evapotranspiration, NASA Goddard Space Flight Center Tech. Memo 83907, 178-180,
798 1981.
799 Morford, S. L., Houlton, B. Z., and Dahlgren, R. A.: Increased forest ecosystem
800 carbon and nitrogen storage from nitrogen rich bedrock, Nature, 477, 78-81, 2011.
801 Neff, J. C., Chapin, F. S., and Vitousek, P. M.: Breaks in the cycle: dissolved
802 organic nitrogen in terrestrial ecosystems, Frontiers in Ecology and the Environment, 1,
803 205-211, doi:10.1890/1540-9295(2003)001[0205:BITCDO]2.0.CO;2, 2003.
804 Nevison, C. D., Esser, G., and Holland, E. A.: A global model of changing N_2O
805 emissions from natural and perturbed soils, Clim. Change, 32, 327-378, 1996.
806 Olivier, J. G. J., Bouwman, A. F., Van der Hoek, K. W., and Berdowski, J. J. M.:
807 Global air emission inventories for anthropogenic sources of NO_x, NH_3 and N_2O in 1990,
808 Environ. Pollut., 102, 135-148, 1998.
809 Parton, W. J., Hartman, M., Ojima, D., and Schimel, D.: DAYCENT and its land
810 surface submodel: description and testing, Global and Planetary Change, 19, 35-48, 1998.

811 Potter, C. S., Matson, P. A., Vitousek, P. M., and Davidson, E. A.: Process
812 modeling of controls on nitrogen trace gas emissions from soils worldwide, J. Geophys.
813 Res., 101, 1361–1377, 1996.
814 Rastetter, E. B., Perakis, S. S., Shaver, G. R., and Agren, G. I.: Terrestrial C
815 sequestration at elevated CO_2 and temperature: the role of dissolved organic N loss, Ecol.
816 Appl., 15, 71-86, doi:10.1890/03-5303, 2005.
817 Ravishankara, A. R., Daniel, J. S., and Portmann, R. W.: Nitrous oxide (N_2O): the
818 dominant ozone-depleting substance emitted in the 21st century, Science, 326, 123-125,
819 10.1126/science.1176985, 2009.
820 Saxton, K. E., Rawls, W. J., Romberger, J. S., and Papendick, R. I.: Estimating
821 generalized soil-water characteristics from texture, Soil Sci. Soc. Am. J., 50, 1031-1036,
822 1986.
823 Schaldac, R., and Pries, J. A.: Integrated Models of the Land System: A Review of
824 Modelling Approaches on the Regional to Global Scale, Living Reviews in Landscape
825 Research, 2, 1-34, 2008.
826 Scheer, C., Wassmann, R., Butterbach-Bahl, K., Lamers, J., and Martius, C.: The
827 relationship between N_2O, NO, and N_2 fluxes from fertilized and irrigated dryland soils
828 of the Aral Sea Basin, Uzbekistan, Plant Soil, 314, 273-283, 2009.
829 Schlesinger, W. H.: On the fate of anthropogenic nitrogen, Proceedings of the
830 National Academy of Sciences, 106, 203-208, 10.1073/pnas.0810193105, 2009.
831 Scholefield, D., Hawkins, J. M. B., and Jackson, S. M.: Development of a helium
832 atmosphere soil incubation technique for direct measurement of nitrous oxide and
833 dinitrogen fluxes during denitrification, Soil Biol. Biochem., 29, 1345-1352, 1997.

834 Seitzinger, S., Harrison, J. A., Böhlke, J. K., Bouwman, A. F., Lowrance, R.,
835 Peterson, B., Tobias, C., and Drecht, G. V.: Denitrification across landscapes and
836 waterscapes: a synthesis, Ecol. Appl., 16, 2064-2090, 2006.
837 Shearer, G., and Kohl, D.: N_2-Fixation in field settings: estimations based on
838 natural ^{15}N abundance, Funct. Plant Biol., 13, 699-756, doi:10.1071/PP9860699, 1986.
839 Shi, S. L., Xing, G. X., Zhou, K. Y., Cao, Y. C., and Yang, W. X.: Natural
840 nitrogen-15 abundance of ammonium nitrogen and fixed ammonium in soils, Pedosphere,
841 2, 265-272, 1992.
842 Sigman, D. M., Robinson, R., Knapp, A. N., van Geen, A., McCorkle, D. C.,
843 Brandes, J. A., and Thunell, R. C.: Distinguishing between water column and
844 sedimentary denitrification in the Santa Barbara Basin using the stable isotopes of nitrate,
845 Geochemistry, Geophysics, Geosystems 4, 1040, doi:1010.1029/2002GC000384, 2003.
846 Sokolov, A. P., Kicklighter, D. W., Melillo, J. M., Felzer, B. S., Schlosser, C. A.,
847 and Cronin, T. W.: Consequences of considering carbon-nitrogen interactions on the
848 feedbacks between climate and the terrestrial carbon cycle, Journal of Climate, 21, 3776-
849 3796, Doi 10.1175/2008jcli2038.1, 2008.
850 Stehfest, E., and Bouwman, L.: N_2O and NO emission from agricultural fields and
851 soils under natural vegetation: summarizing available measurement data and modeling of
852 global annual emissions, Nutr. Cycl. Agroecosyst., 74, 207-228, 2006.
853 Sutka, R. L., Ostrom, N. E., Ostrom, P. H., Breznak, J. A., Gandhi, H., Pitt, A. J.,
854 and Li, F.: Distinguishing nitrous oxide production from nitrification and denitrification
855 on the basis of isotopomer abundances, Appl. Environ. Microbiol., 72, 638-644,
856 10.1128/aem.72.1.638-644.2006, 2006.

857 Swerts, M., Uytterhoeven, G., Merckx, R., and Vlassak, K.: Semicontinuous
858 measurement of soil atmosphere gases with gas-glow soil core method, Soil Sci. Soc. Am.
859 J., 59, 1336-1342, 1995.
860 Thornton, P. E., Doney, S. C., Lindsay, K., Moore, J. K., Mahowald, N., Randerson,
861 J. T., Fung, I., Lamarque, J. F., Feddema, J. J., and Lee, Y. H.: Carbon-nitrogen
862 interactions regulate climate-carbon cycle feedbacks: results from an atmosphere-ocean
863 general circulation model, Biogeosciences, 6, 2099-2120, 2009.
864 Vitousek, P. M.: Litterfall, Nutrient Cycling, and Nutrient Limitation in Tropical
865 Forests, Ecology, 65, 285-298, doi:10.2307/1939481, 1984.
866 Wang, Y.-P., and Houlton, B. Z.: Nitrogen constraints on terrestrial carbon uptake:
867 Implications for the global carbon-climate feedback, Geophys. Res. Lett., 36,
868 10.1029/2009gl041009, 2009.
869 Wang, Y. P., Houlton, B. Z., and Field, C. B.: A model of biogeochemical cycles of
870 carbon, nitrogen, and phosphorus including symbiotic nitrogen fixation and phosphatase
871 production, Global Biogeochemical Cycles, 21, doi:10.1029/2006GB002797, 2007.
872 Wang, Y. P., Law, R. M., and Pak, B.: A global model of carbon, nitrogen and
873 phosphorus cycles for the terrestrial biosphere, Biogeosciences, 7, 2261-2282, 2010.
874 Wellman, R. P., Cook, F. D., and Krouse, H. R.: Nitrogen-15: microbiological
875 alteration of abundance, Science, 161, 269-270, 10.1126/science.161.3838.269, 1968.
876 Whitehead, P. G., Wilson, E. J., and Butterfield, D.: A semi-distributed ntegrated
877 itrogen model for multiple source assessment in tchments (INCA): Part I -- model
878 structure and process equations, Sci. Total Environ., 210-211, 547-558, 1998.

879 Williams, J. R., Jones, C. A., and Dyke, P. T.: A modeling approach to determining
880 the relationship between erosion and soil productivity, Transactions of the ASAE 17,
881 129-144, 1984.
882 Willmott, C. J., and Matsuura, K.: Terrestrial Air Temperature and Precipitation:
883 Monthly and Annual Climatologies, Version 3.01, 2000.
884 Wolf, I., and Brumme, R.: Dinitrogen and nitrous oxide formation in beech forest
885 floor and mineral soils, Soil Sci. Soc. Am. J., 67, 1862-1868, 2003.
886 Xu, X., Tian, H., and Hui, D.: Convergence in the relationship of CO_2 and N_2O
887 exchanges between soil and atmosphere within terrestrial ecosystems, Global Change
888 Biology, 14, 1651-1660, 2008.
889 Yan, X., Ohara, T., and Akimoto, H.: Statistical modeling of global soil NO_x
890 emissions, Global Biogeochem. Cycles, 19, doi:10.1029/2004GB002276, 2005.
891 Yienger, J. J., and Levy, H., II: Empirical model of global soil-biogenic NO_x
892 emissions, Journal of Geophysical Research - Atmospheres 100, 11447-11464, 1995.
893 Yoneyama, T., Fujita, K., Yoshida, T., Matsumoto, T., Kambayashi, I., and Yazaki,
894 J.: Variation in natural abundance of ^{15}N among plant parts and in $^{15}N/^{14}N$ fractionation
895 during N_2 fixation in the legume-rhizobia symbiotic system, Plant Cell Physiol., 27, 791-
896 799, 1986.
897 Yoshida, N.: ^{15}N-depleted N_2O as a product of nitrification, Nature, 335, 528-529,
898 1988.
899 Zaehle, S., Friedlingstein, P., and Friend, A. D.: Terrestrial nitrogen feedbacks may
900 accelerate future climate change, Geophysical Research Letters, 37, L01401, 2010a.

Zaehle, S., Friend, A. D., Friedlingstein, P., Dentener, F., Peylin, P., and Schulz, M.: Carbon and nitrogen cycle dynamics in the O-CN land surface model: 2. Role of the nitrogen cycle in the historical terrestrial carbon balance, Global Biogeochemical Cycles, 24, GB1006, 2010b.

Figure Legends

Figure 1 Diagram of N cycling and its influences on global change.

Figure 2. Model structure.

Figure 3. Model of N gas production as a function of WFPS (water-filled pore space, %). The solid line represents NO; short dash line represents N_2O fraction; and long dash line represents N_2.

Figure 4. Comparison of the ratios of N_2O-N/(N_2O-N+NO-N) and N_2O-N/(N_2O-N+N_2-N) from field measurements (points) with ratios predicted by the gas partitioning model (lines). Additional information on the field measurements is presented in Supplementary Table 1.

Figure 5. Comparison of modelled soil NO emissions (g N m^{-2} $month^{-1}$) (a) with space-based observations of NO_2 column concentrations (10^{15} molecules cm^{-2}) as reported in ref (Jaegle *et al.*, 2004) (b) and fire counts (c) as observed by the visible and infrared scanner on board the TRMM satellite (Jaegle *et al.*, 2004) over Africa for January, June and August, 2000. The pink rectangular shows the area with unexpectedly high level of NO_2 (b) during June , which was not caused by fire or industrial emissions based on the fire count map (c); rather, soil

923 microbial NO_x pulses following the onset of rainfall over vast areas of dry soil, a
924 notion confirmed by our model simulations (a).

925 Figure 6. Sensitivity of denitrification to different input parameters. "+" and "-
926 " represent a 10% increase and 10% decrease in the input parameter, respectively.

927 Figure 7. Global patterns of fraction of gaseous N losses (f_{gas}) (a), total gaseous N flux (b),
928 and total leaching N flux (c) from un-managed soils.

929 Figure 8. Global patterns of NO (a), N_2O (b), and N_2 (c) from un-managed soils.

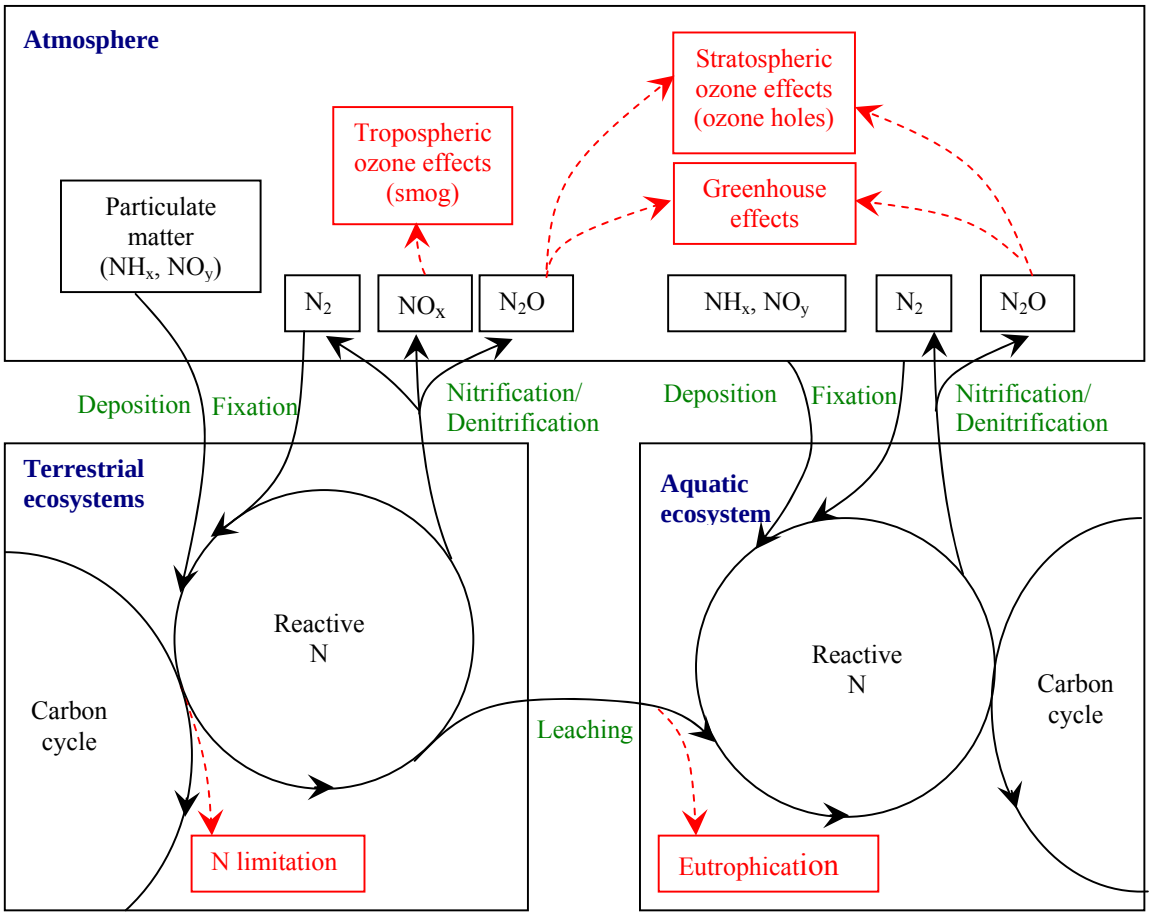
Atmosphere
Stratospheric ozone effects (ozone holes)
Tropospheric ozone effects (smog)
Greenhouse effects
Particulate matter (NH_x, NO_y)
N_2
NO_x
N_2O
NH_x, NO_y
N_2
N_2O
Deposition
Fixation
Nitrification/ Denitrification
Deposition
Fixation
Nitrification/ Denitrification
Terrestrial ecosystems
Aquatic ecosystem
Reactive N
Carbon cycle
Leaching
Reactive N
Carbon cycle
N limitation
Eutrophication

Fig. 1

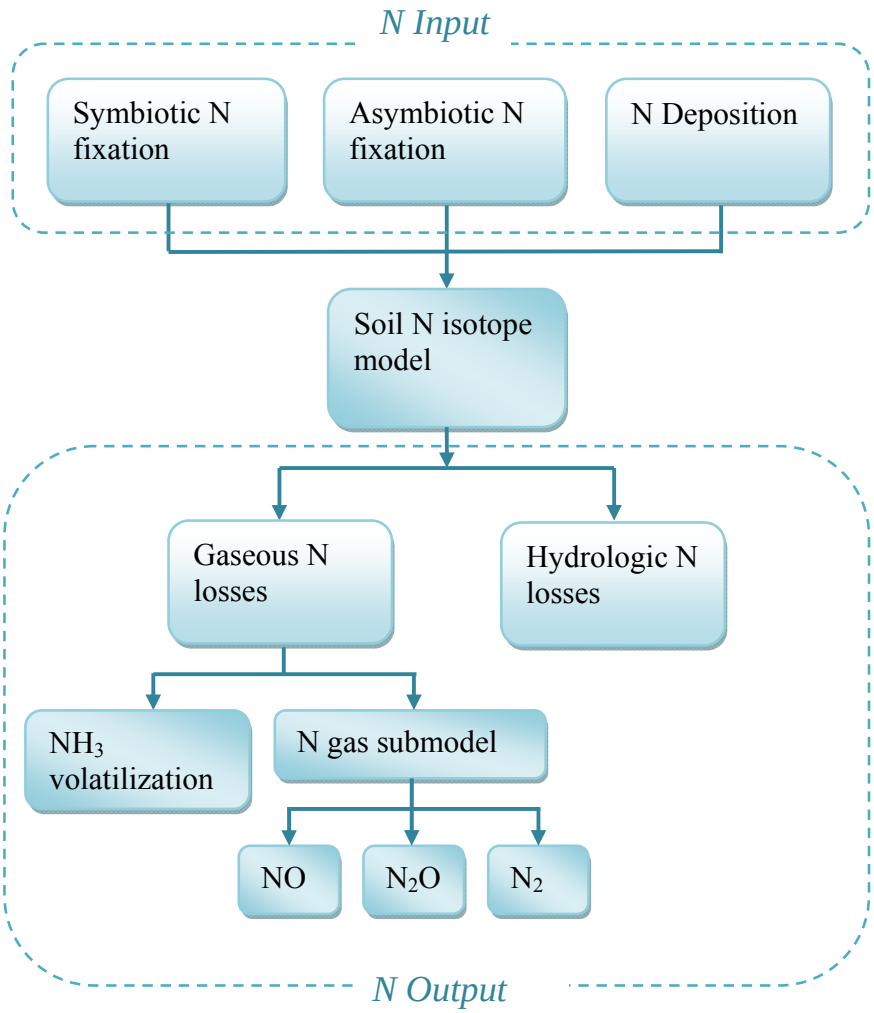
N Input
Symbiotic N fixation
Asymbiotic N fixation
N Deposition
Soil N isotope model
Gaseous N losses
Hydrologic N losses
NH3 volatilization
N gas submodel
NO
N2O
N2
N Output

Fig. 2

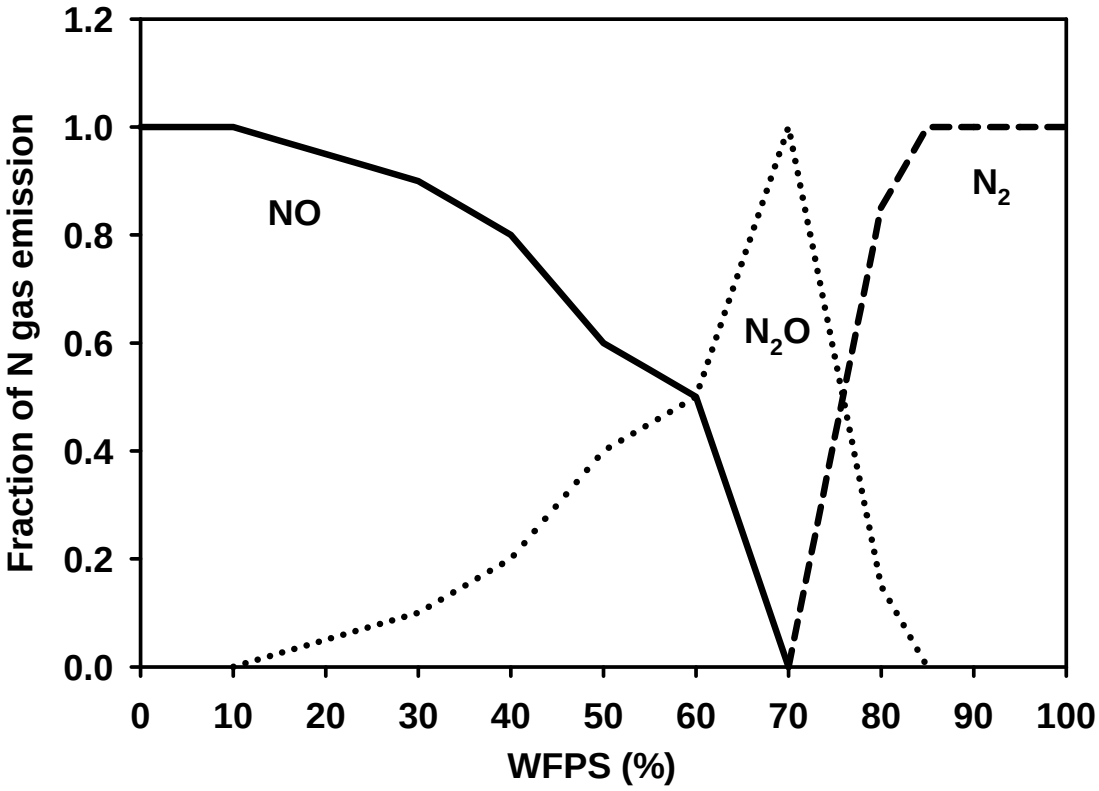

952

953 Fig. 3

954

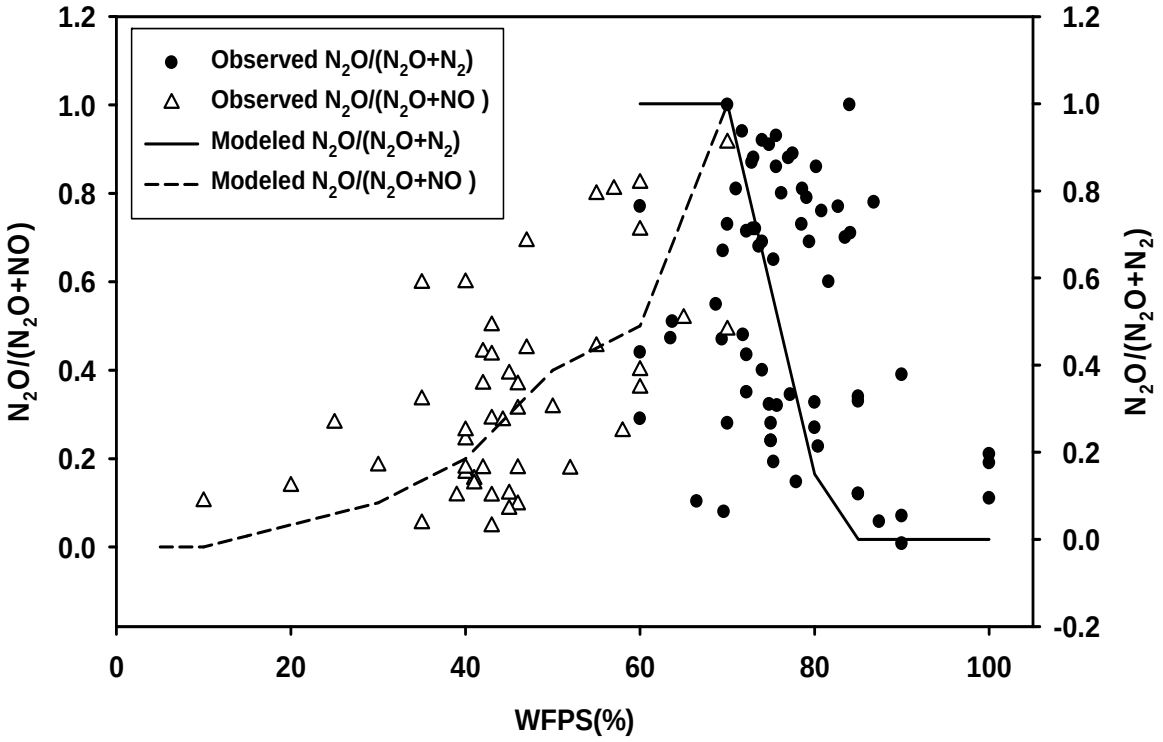

955
956

957 Fig. 4

958

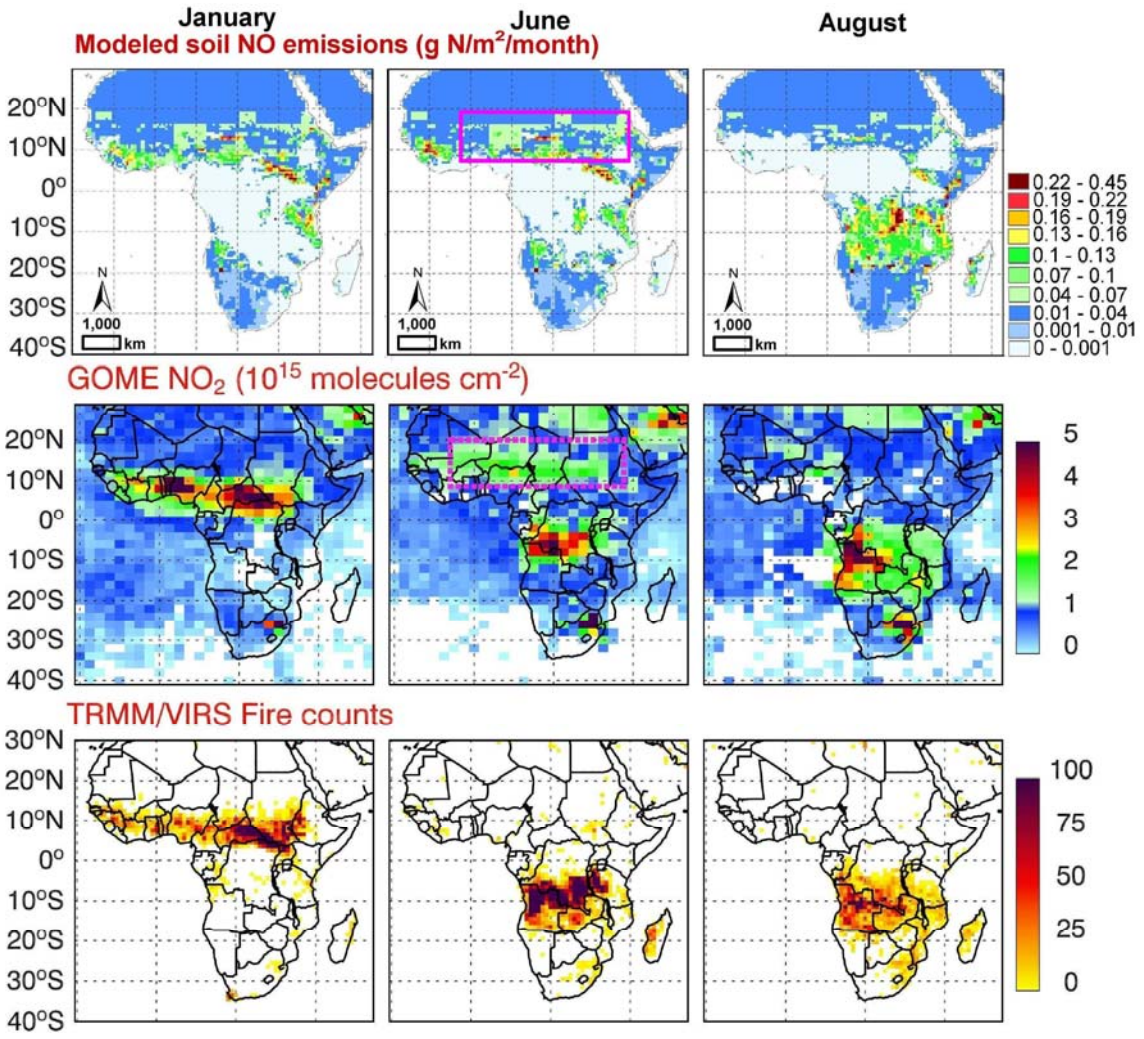
January
June
August
Modeled soil NO emissions (g N/m²/month)
20°N
10°N
0°
10°S
20°S
30°S
40°S
N
1,000 km
0.22 - 0.45
0.19 - 0.22
0.16 - 0.19
0.13 - 0.16
0.1 - 0.13
0.07 - 0.1
0.04 - 0.07
0.01 - 0.04
0.001 - 0.01
0 - 0.001
GOME NO2 (10^15 molecules cm^-2)
5
4
3
2
1
0
TRMM/VIRS Fire counts
30°N
100
75
50
25
0

959

960 Fig. 5

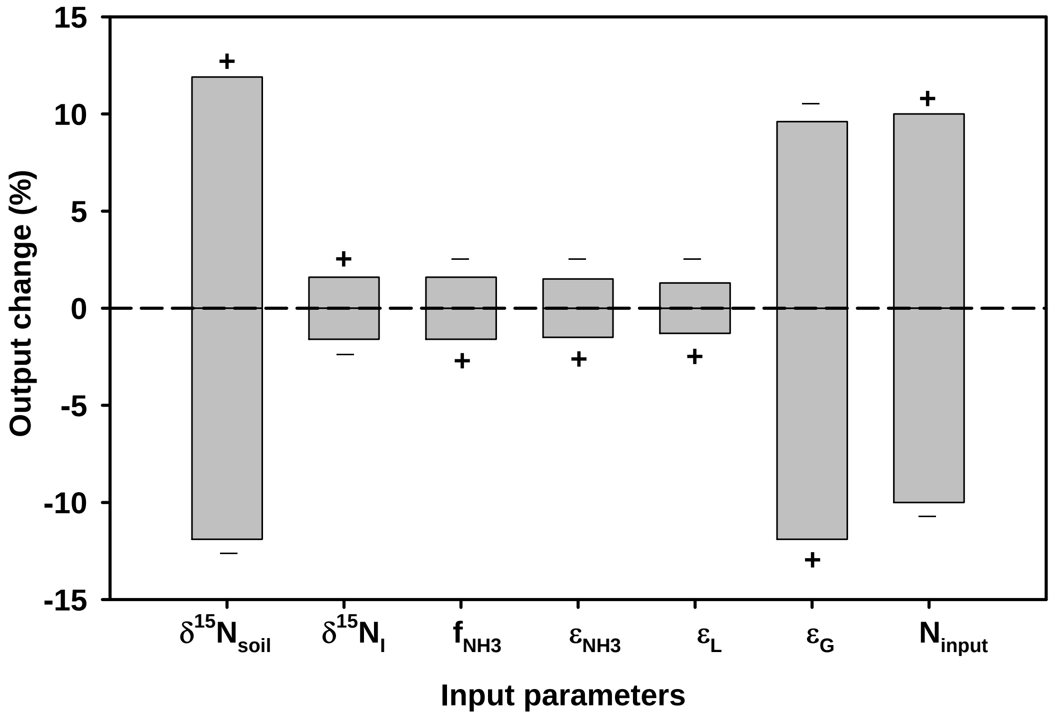
Output change (%)
15
10
5
0
-5
-10
-15
δ15Nsoil
δ15Nl
fNH3
εNH3
εL
εG
Ninput
Input parameters

Fig. 6

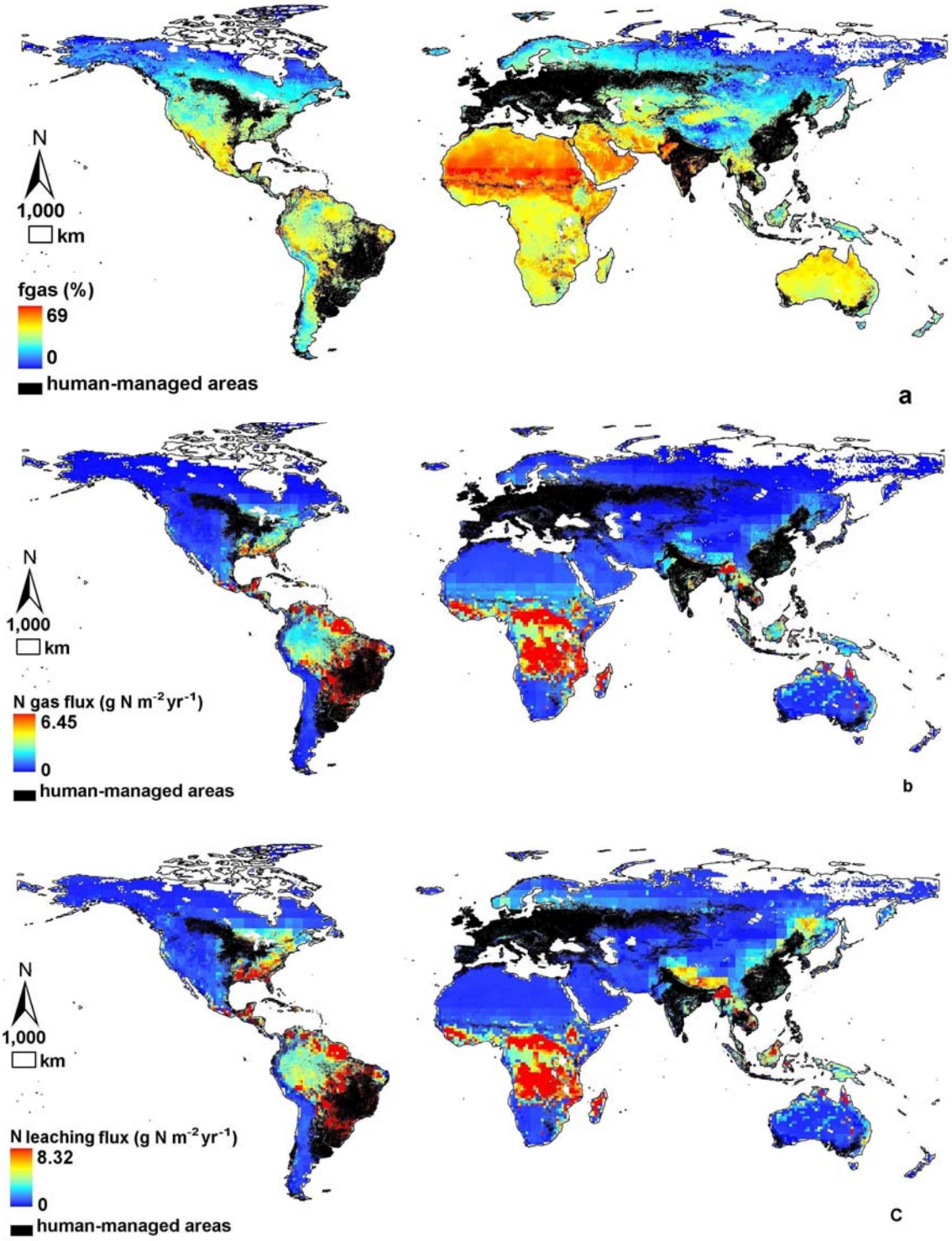
N
1,000
km
fgas (%)
69
0
human-managed areas
a
N
1,000
km
N gas flux (g N m-2 yr-1)
6.45
0
human-managed areas
b
N
1,000
km
N leaching flux (g N m-2 yr-1)
8.32
0
human-managed areas
c

964

965 Fig. 7

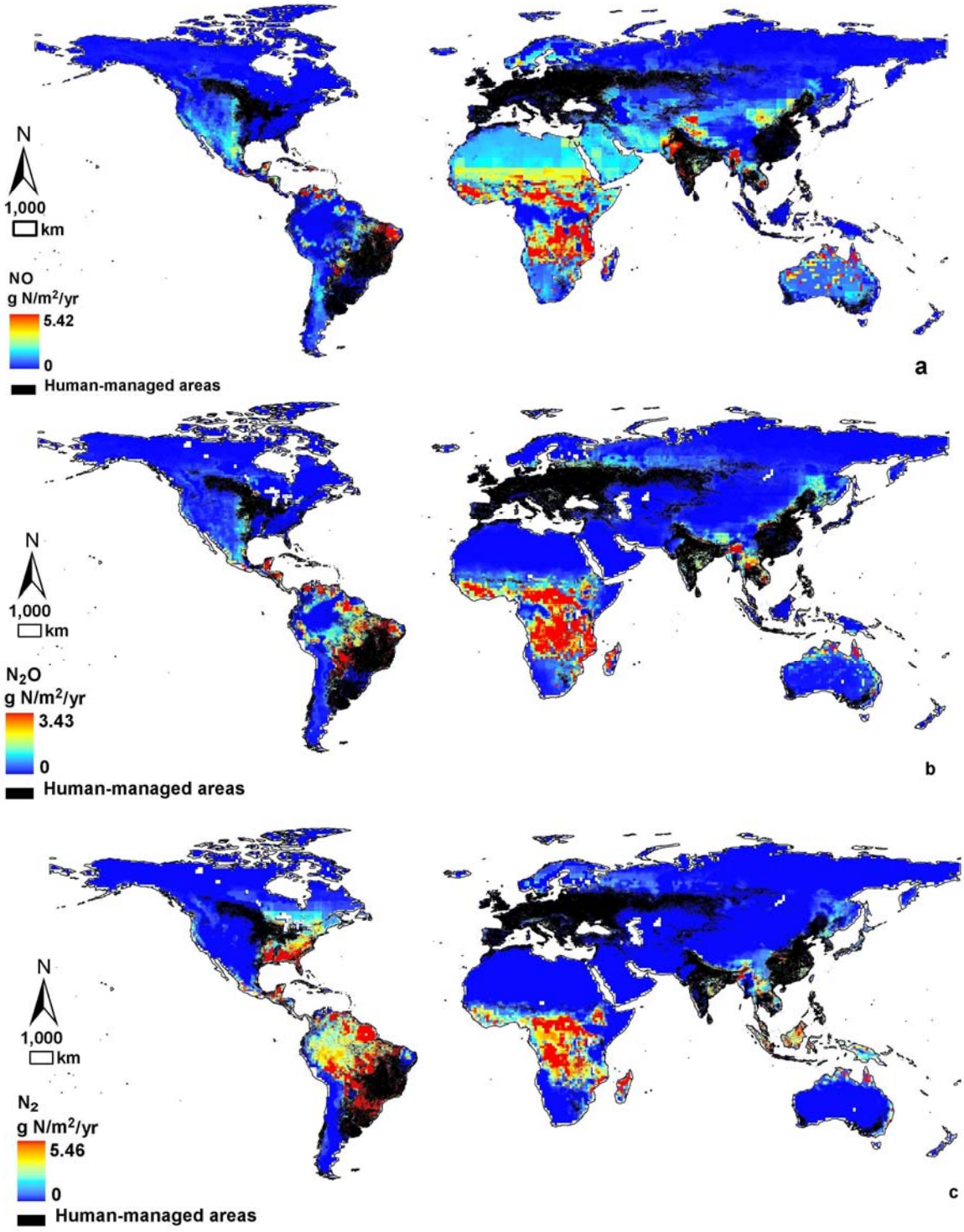

966

967 Fig. 8

968

969 **Tables**

970 Table 1 Comparison of global estimations of N gas productions by N isotope model with
971 previously published empirical and modelling studies (NO fluxes are soil-surface
972 emissions without canopy effects).

Sources	Area (10^{12} m^2)	NO (Tg N yr^{-1})	N_2O (Tg N yr^{-1})	N_2 (Tg N yr^{-1})	Method	Reference
Natural	103.5	11.2-20.3	7.2-13.2	14.9-27.1	N isotope model	this study
	114.0	9.1-16.0			statistical modelling	(Davidson and Kingerlee, 1997)
	97.7	5.02			statistical modelling	(Yan *et al.*, 2005)
	NR	7.22			statistical modelling	(Yienger and Levy, 1995)
	99.2	5.44			statistical modelling	(Lee *et al.*, 1997)
	NR	3.0-8.0			IPCC assessment	(Denman *et al.*, 2007)
	NR		3.3-9.9		IPCC assessment	(Ehhalt *et al.*, 2001)
	118.2		6.0		statistical modelling	(Bouwman *et al.*, 1995)
	NR		5.73-12.90		statistical modelling	(Xu *et al.*, 2008)
	135.2		10.7		statistical modelling	(Dalal and Allen, 2008)
	NR	5.0-26.0	7.0-16.0		statistical modelling	(Bowden, 1986)
	122.2	7.69	5.02		process-based modelling	(Potter *et al.*, 1996)
	NR		6.2		process-based modelling	(Nevison *et al.*, 1996)
Agricul-tural	16.0	3.9-5.5			statistical modelling	(Davidson and Kingerlee, 1997)
	14.5	2.41			statistical modelling	(Yan *et al.*, 2005)
	NR	2.98			statistical modelling	(Yienger and Levy, 1995)
	17.6	5.55			statistical modelling	(Lee *et al.*, 1997)
	NR	0-4.0			IPCC summary	(Denman *et al.*, 2007)
	NR		1.9-4.2		IPCC summary	(Ehhalt *et al.*, 2001)
	14.4		0.4		statistical modelling	(Bouwman *et al.*, 1995)
	NR		2.46-5.53		statistical modelling	(Xu *et al.*, 2008)
	19.06	1.8	4.1		statistical modelling	(Stehfest and Bouwman, 2006)
	13.1	2.00	1.10		process-based modelling	(Potter *et al.*, 1996)
	NR		2.58		process-based modelling	(Nevison *et al.*, 1996)
All	NR		11.33		process-based modelling	(Liu, 1996)
	NR		8.3-15.0		inverse modelling	(Hirsch *et al.*, 2006)
	NR		11.0-14.4		inverse modelling	(Huang *et al.*, 2008)

973 NR: Not reported

974 Table 2. Modeled results of regional N gas fluxes from soil denitrification.

Region	Area (10^{12} m^2)	Modeled N gas flux (g $N/m^2/yr$)		
		NO	N_2O	N_2
Closed tropical forest	9.0	0.099-0.229	0.180-0.418	0.602-1.396
Tropical rainforests	9.2	0.095-0.217	0.176-0.400	0.610-1.390
Tropical savanna /woodland	17.6	0.267-0.711	0.150-0.398	0.210-0.560
Brazilian Amazon forest	5.5	0.067-0.285	0.129-0.553	0.406-1.734
Grassland/ steppe	22.3	0.101-0.179	0.037-0.065	0.028-0.050
Temperate/ boreal forest	21.1	0.023-0.055	0.029-0.069	0.104-0.244
Deserts and semi-deserts	16.2	0.120-0.266	0.003-0.007	0.001-0.003
Chihuahuan Desert	0.005	0.020-0.323	0.003-0.049	0.000
Tundra	10.7	0.000-0.007	0.000-0.007	0.000-0.010
Africa (18˚ N - 30˚ S)	16.0	0.213-0.657	0.165-0.507	0.239-0.737
European forest	3.0	0.026-0.118	0.042-0.184	0.038-0.162
United States	5.33	0.023-0.119	0.008-0.044	0.106-0.544

975